

## Early Oligocene Siliceous Microfossil Biostratigraphy of Cape Roberts Project Core CRP-3, Victoria Land Basin, Antarctica

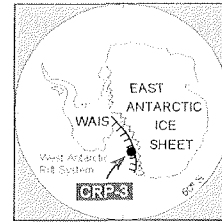
D.M. HARWOOD<sup>1\*</sup> & S.M. BOHATY<sup>2</sup>

<sup>1</sup>Department of Geosciences, University of Nebraska-Lincoln, Lincoln, NE 68588-0340 - USA

<sup>2</sup>Earth Sciences Department, University of California, Santa Cruz, CA 95064 - USA

Received 29 October 2000; accepted in revised form 19 November 2001

**Abstract** - Early Oligocene siliceous microfossils were recovered in the upper *c.* 193 m of the CRP-3 drillcore. Although abundance and preservation are highly variable through this section, approximately 130 siliceous microfossil taxa were identified, including diatoms, silicoflagellates, ebridians, chrysophycean cysts, and endoskeletal dinoflagellates. Well-preserved and abundant assemblages characterize samples in the upper *c.* 70 m and indicate deposition in a coastal setting with water depths between 50 and 200 m. Abundance fluctuations over narrow intervals in the upper *c.* 70 mbsf are interpreted to reflect environmental changes that were either conducive or deleterious to growth and preservation of siliceous microfossils. Only poorly-preserved (dissolved, replaced, and/or fragmented) siliceous microfossils are present from *c.* 70 to 193 mbsf. Diatom biostratigraphy indicates that the CRP-3 section down to *c.* 193 mbsf is early Oligocene in age. The lack of significant changes in composition of the siliceous microfossil assemblage suggests that no major hiatuses are present in this interval. The first occurrence (FO) of *Cavitatus jouseanus* at 48.44 mbsf marks the base of the *Cavitatus jouseanus* Zone. This datum is inferred to be near the base of Subchron C12n at *c.* 30.9 Ma. The FO of *Rhizosolenia antarctica* at 68.60 mbsf marks the base of the *Rhizosolenia antarctica* Zone. The FO of this taxon is correlated in deep-sea sections to Chron C13 (33.1 to 33.6 Ma). However, the lower range of *R. antarctica* is interpreted as incomplete in the CRP-3 drillcore, as it is truncated at an underlying interval of poor preservation; therefore, an age of *c.* 33.1 to 30.9 Ma is inferred for interval between *c.* 70 and 50 mbsf. The absence of *Hemiaulus characteristicus* from diatom-bearing interval of CRP-3 further indicates an age younger than *c.* 33 Ma (Subchron C13n) for strata above *c.* 193 mbsf. Siliceous microfossil assemblages in CRP-3 are significantly different from the late Eocene assemblages reported CIROS-1 drillcore. The absence of *H. characteristicus*, *Stephanopyxis splendidus*, and *Pterotheca danica*, and the ebridians *Ebriopsis crenulata*, *Parebriopsis fallax*, and *Pseudanmodochium dictyoides* in CRP-3 indicates that the upper 200 m of the CRP-3 drillcore is equivalent to part of the stratigraphic interval missing within the unconformity at *c.* 366 mbsf in CIROS-1.



### INTRODUCTION

Cape Roberts Project drillcore CRP-3 is the third in a series of drillcores that sampled eastward dipping strata on the western edge of the Victoria Land Basin, Ross Sea, Antarctica. Cores CRP-1, CRP-2/2A, and CRP-3 represent a composite section of *c.* 1500 m through lower Miocene to lower Oligocene strata. Combined, these drillcores provide a proxy record of climate and sea level change between *c.* 17 and 33 Ma on the Ross Sea margin of East Antarctica. These strata were deposited in a marine environment, and consist largely of clastic sediment that exhibits influence from cyclic sedimentation thought to be a result of both glacio-eustatic variation and local glacial advance and retreat. The recovery of this composite section enables the development of a biostratigraphic framework for the lower Oligocene through lower Miocene based on siliceous microfossils (marine diatoms, silicoflagellates,

ebridians, chrysophycean cysts and endoskeletal dinoflagellates). Calibration of siliceous microfossil datums to the magnetic polarity time scale will advance future age determinations of the Oligocene and Miocene on the Antarctic shelf.

The CRP-3 site is located 12 km east of Cape Roberts (77.01°S, 163.64°E) at 295 m water depth. The CRP-3 drillhole was cored from a depth of 2.80 to 939.42 mbsf with 97% recovery. Glacimarine strata between *c.* 3 and 823 mbsf were tentatively dated as early Oligocene in age, although a latest Eocene age is possible for the lower part of this section based on magnetic polarity data (Cape Roberts Science Team, 2000; Florindo et al., this volume). Sediment-accumulation rates were most likely high through this section; the chronology of the CRP-2/2A drillcore (Wilson et al., 2000) identifies Oligocene accumulation rates that approach and likely exceed 1000 m/m.y. Beacon Sandstone of mid Devonian age underlies the Palaeogene strata of CRP-3 between

\*Corresponding author (dharwood@unlserve.unl.edu)

Tab. 1 - Relative abundance of siliceous microfossils in the upper 100 m of CRP-3. \* = sedimentary clast sample.

Upper Sample Depth	Lower Sample Depth	Abund-ance	Upper Sample Depth	Lower Sample Depth	Abund-ance	Upper Sample Depth	Lower Sample Depth	Abund-ance
2.85	2.86	R	36.61	36.63	C	59.66	59.67	C
3.05	3.06	F*	37.29	37.30	A	60.13	60.14	F
5.01	5.02	C	37.71	37.73	A	61.10	61.11	C
6.87	6.88	C	38.78	38.79	C	61.70	61.71	C
7.85	7.86	A	39.34	39.35	C	62.12	62.13	A
8.15	8.16	C	39.35	39.36	A	62.46	62.47	A
8.88	8.89	C	40.63	40.64	R	62.98	62.99	A
9.69	9.70	C	41.00	41.01	C	63.64	63.65	C
10.48	10.49	R	41.75	41.76	C	64.04	64.05	F
10.78	10.79	C	41.76	41.77	T	64.44	64.45	C
11.12	11.13	C	43.09	43.10	A	64.57	64.58	F
11.63	11.64	C	43.10	43.13	C	64.93	64.94	T
12.19	12.20	A	43.70	43.72	F	65.90	65.91	F
12.64	12.65	A	43.72	43.73	C	66.16	66.17	F
13.72	13.73	A	44.18	44.27	F	66.56	66.57	R
14.28	14.29	F	44.50	44.52	C	66.70	66.71	F
14.46	14.47	C	44.93	44.94	F	68.59	68.60	T
15.68	15.69	T	45.63	45.64	F	70.60	70.61	R
15.99	16.00	F	46.04	46.05	R	71.27	71.28	T
17.82	17.83	T	46.42	46.43	C	71.54	71.55	T
18.02	18.03	R	46.84	46.85	R	72.89	72.91	T
18.19	18.20	T	47.60	47.61	F	73.61	73.62	T
19.10	19.11	T	47.87	47.88	A	74.93	74.94	T
19.62	19.63	T	48.43	48.44	F	76.08	76.09	T
20.46	20.47	T	48.44	48.45	F	77.11	77.12	T
21.36	21.37	T	49.67	49.68	A	77.80	77.81	T
22.12	22.13	T	50.47	50.48	C	80.33	80.34	T
22.26	22.27	F	50.89	50.90	A	80.91	80.92	T
22.75	22.76	T	51.56	51.57	C	81.98	81.99	T
24.20	24.21	R	52.54	52.55	F	82.34	82.35	T
25.08	25.09	B	52.91	52.92	R	83.04	83.05	T
25.94	25.95	T	54.19	54.20	A	85.46	85.47	T
26.72	26.73	T	54.54	54.55	A	87.14	87.15	T
28.44	28.45	R	54.77	54.78	A	88.18	88.19	R*
28.70	28.71	R	55.66	55.67	A	89.25	89.26	T
30.50	30.51	T	56.16	56.17	C	90.86	90.87	T
32.20	32.21	F	56.84	56.85	A	91.91	91.92	B
32.51	32.52	T	57.71	57.72	A	92.94	92.95	T
33.21	33.22	T	57.80	57.81	A	93.52	93.53	T
33.95	33.96	F	58.95	58.96	C	96.06	96.07	T
34.57	34.58	R	59.21	59.22	A	98.13	9.14	T
35.70	35.71	C						

contains only trace to rare diatoms. Only rare, poorly preserved assemblages are present in the interval between 71.3 and 193.2 mbsf, and all samples below 193.2 mbsf are barren.

Approximately 120 marine diatom taxa, 6 silicoflagellate taxa, 8 ebridian and other siliceous flagellate taxa, and 3 chrysophyte cyst taxa were identified in the rich interval of siliceous microfossils above *c.* 70 mbsf (Tab. 2). This upper interval corresponds to Lithostratigraphic Units (LSU) 1.1, 1.2, and 1.3 (2.85 to 66.71 mbsf) (Cape Roberts Science Team, 2000). Many samples in this section contain a high species richness of siliceous microfossil taxa (Fig. 1), and excellent preservation is exemplified by the presence of articulated valves of *Pyxilla* spp. and *Eurossia irregularis* (see Plate 3, Figs. 1-3; Plate 4, Figs. 1, 2, 5, 8).

Poorly-preserved diatom specimens between 193 and 85 mbsf are commonly etched, fragmented, or replaced (*i.e.* silicified casts are present). Assemblages in this interval have undergone significant diagenetic alteration and are interpreted to represent "residual" assemblages that were once rich in siliceous

microfossils (*e.g.* *c.* 120-130 mbsf and *c.* 190-195 mbsf). Although the section currently resides at relatively shallow seafloor depths, prior burial at much deeper levels may have resulted in extensive opal dissolution.

### CRP-3 BIOSTRATIGRAPHY

Several diatom taxa present in CRP-3 assemblages are well-documented in Southern Ocean drillcores (Harwood & Maruyama, 1992). As discussed above, however, most Southern Ocean taxa, are rare in CRP-3 and occur sporadically. Until a biozonation is developed for Antarctic shelf sediments, correlation and age control for CRP-3 must be derived through linkage to the Southern Ocean diatom biostratigraphy.

In CRP-3, the first occurrence (FO) of *Cavitatus jouseanus* occurs between 48.44 and 49.68 mbsf and marks the base of the *Cavitatus jouseanus* Zone of Scherer et al. (2000). The top of this zone is identified by the last occurrence (LO) of *Rhizosolenia antarctica*, which is noted in the CRP-2A drillcore at a depth of 441.85 mbsf (Scherer et al., 2000).

Tab. 2 - Relative abundance and occurrence data for selected siliceous microfossil taxa in the upper 200 metres of CRP-3. Ecology notes column reflects the occurrence of ecological diatom groups: n = neritic; b = benthic; Ch. = *Chaetoceros* rich. Codes for the table are indicated in the Methods section of the text. Drillcores listed in brackets indicate the origin of informal taxonomic designations: MSSTS-1 = Harwood (1986); CIROS-1 = Harwood (1989); 739C = Barron and Mahood (1993); CRP-2/2A = Scherer et al. (2000); and CRP-3 = this paper.

Upper Depth (mbsf)	Lower Depth (mbsf)	Ecology notes	Diatom Species Richness	Diatoms
2.85	2.86		12	<i>Actinocyclus senarius</i>
3.05	3.06-1		24	<i>Aviculus</i> sp.
5.01	5.02		43	<i>Arachnoidiscus</i> spp.
6.87	6.88		24	<i>Asteromphalus punctifer</i>
7.85	7.86		50	<i>Asteromphalus oligocenicus</i>
8.15	8.16	n,b	32	<i>Autocidiscus</i> spp.
9.69	9.70		29	<i>Biddulphia tuomeyi</i> group [CIROS-1]
10.78	10.79		48	<i>Biddulphia</i> sp. A [CIROS-1]
12.64	12.65		30	<i>Cavitatus jouseanus</i>
13.72	13.73		35	<i>Cavitatus</i> sp. cf. <i>C. nitescens</i>
14.46	14.47		33	<i>Chaetoceros</i> spp. groups A, B, C [CRP-2/2A]
22.26	22.27		27	<i>Chaetoceros</i> sp. [MSSTS-1]
24.20	24.21		8	<i>Chaetoceros</i> resting sp. A [739C]
25.94	25.95		7	<i>Chaetoceros pandoraefornis</i>
28.44	28.45		32	<i>Cocconeis</i> spp.
28.70	28.71		40	<i>Cocconeis</i> spp.
32.20	32.21	Ch	27	<i>Diploneis</i> spp.
33.95	33.96	b	38	<i>Enrosia irregularis</i> var. <i>irregularis</i>
34.57	34.58		18	<i>Goniolobium decoratum</i>
36.61	36.63		43	<i>Goniolobium edmontella</i>
37.29	37.30		42	<i>Grammatophora</i> sp.
38.78	38.79		45	<i>Hemiaulus</i> spp.
39.34	39.35		49	<i>Hemiaulus</i> sp. cf. <i>nitra</i>
41.00	41.01		42	<i>Hemiaulus polycystinorum</i>
43.70	43.71	n,b	38	<i>Hemiaulus rectus</i> var. <i>novus</i>
44.18	44.27	b	44	<i>Hemiaulus</i> sp. B [CRP-2/2A]
44.93	44.94		36	<i>Hemiaulus</i> sp. D [CRP-3]
46.84	46.85		29	<i>Ikebea</i> sp. A [CRP-2/2A]
48.43	48.44		37	<i>Ikebea</i> sp. B [CRP-2/2A]
49.67	49.68		34	<i>Ikebea</i> sp. D [CRP-3]
50.47	50.48		30	<i>Isahia</i> spp.
51.56	51.57		41	<i>Kannoa hastata</i>
54.19	54.20		46	<i>Kisselevella</i> sp. C [CRP-2/2A]
54.77	54.78		48	<i>Kisselevella</i> sp. D [CRP-2/2A]
56.16	56.17		29	<i>Kisselevella</i> sp. F [CRP-2/2A]
57.71	57.72		34	<i>Kisselevella</i> sp. G [CRP-2/2A]
59.66	59.67		30	<i>Kisselevella</i> sp. H [CRP-3]
61.70	61.71		39	<i>Liriodiscus ovalis</i>
62.46	62.47	b	33	<i>Navicula</i> ? spp.
62.98	62.99	n,b	33	<i>Olomella fibriata</i>
63.64	63.65		25	<i>Paralia sal.</i> var. <i>marginalis</i>
64.44	64.45	b	30	<i>Paralia salicata</i>
65.90	65.91	b	26	
66.70	66.71	b	23	
68.59	68.60		13	
70.60	70.61		18	
71.27	71.28		6	
72.89	72.91		5	
73.61	73.62		5	
77.80	77.81		5	
81.98	81.99		4	
82.34	82.35		2	
101.03	101.04		1	
104.62	104.63		8	
107.37	107.38		6	
123.65	123.73		7	
127.11	127.12		13	
157.75	157.76		7	
190.81	190.82		12	
193.16	193.17		7	
195.58	195.59		3	

The age of the FO of *Cavitatus jouseanus* has been determined at several Southern Ocean sites, but is applied in the present study with some caution. In ODP Hole 748B (Kerguelen Plateau), this datum occurs within the lower part of the calcareous nannofossil *Chiasmolithus altus* Zone, within Subchron C12n (Harwood & Maruyama, 1992; Harwood et al., 1992; Wei & Wise, 1992). The age of

this datum is inferred from a position near the base of C12n at ~30.9 Ma (using the time scale of Berggren et al., 1995). The FO of *C. jouseanus* in ODP Hole 744A (Kerguelen Plateau) also occurs within the lower part of the calcareous nannofossil *Chiasmolithus altus* Zone, near the boundary between Subchrons C12n and C12r (Baldauf & Barron, 1991; Barron et al., 1991, Fig. 10). Fenner (1984)



Tab. 2 - Continued.

Upper Depth (mbsf)	Lower Depth (mbsf)	Sitotidicus hermannianus Sitotidicus ? klitoniensis Thalassiosira ? mediacoxeana Triceratium pulvinar Trigoniium arcticum Triacria excavata Triacria racovitzae Trochostira spinosus Valonella homae Genus et sp. indet. A [CIROS-1] Genus et sp. indet. B [CIROS-1] Genus et sp. indet. C [CIROS-1] Genus et sp. indet.	Silicoflagellates Corbisema apiculata apiculata Corbisema triacantha Dityocha deflandrei Dityocha frenguelli Dityocha spp. Discophanus erux Discophanus rampii	Ehrharians and other siliceous flagellates Ammodendrium rectangulare A. rectangulare (double w/ medial silicification) Calcepedinium sp. A [CRP-2,2A] Ehrharia paradoxica Falsebria ambigua H. brevispinosa group Macrurusippium cf. caricatum Pyxid. sphericum s.l. (single/double) Cordiaphelia gracilis	Chrysophyte cysts Chrysophyte cysts Archaeosphaeridium australensis Archaeosphaeridium tasmaniae Archaeomonas edwardsii	Additional Taxa Fecal pellets clumps of Chaetoceros	Diatom Zonation
2.85	2.86						
3.05	3.06 cl.						
5.01	5.02	R	R	X			
6.87	6.88	fr	R	R			
7.85	7.86	R	R	R			
8.15	8.16	X	R	R			
9.69	9.70			X			
10.78	10.79	R	R	R			
12.64	12.65			X			
13.72	13.73	fr	R	R			
14.46	14.47	R	R	R			
22.26	22.27	R		R			
24.20	24.21	X		R			
25.94	25.95			R			
28.44	28.45	X	X	R			
28.70	28.71	R X	R	R X			
32.20	32.21			R			
33.95	33.96	R	R	R			
34.57	34.58			R			
36.61	36.63	X R F	X	R			
37.29	37.30	R	X	R			
38.78	38.79	R	X	R			
39.34	39.35	X R	X	R			
41.00	41.01	X R	X	R			
43.70	43.71	R	R	R			
44.18	44.27	X X X	X	R R			
44.93	44.94	X X X	X	R R			
46.84	46.85	X R	X	R			
48.43	48.44	R X	R	R			
49.67	49.68	X R R	X	R R			
50.47	50.48	R	R	R R			
51.56	51.57			R			
54.19	54.20	r	R	X			
54.77	54.78		F	X			
56.16	56.17			X			
57.71	57.72	R		X			
59.66	59.67			X			
61.70	61.71	R		X			
62.46	62.47	R		X			
62.98	62.99	X	R	X			
63.64	63.65	X	R	X			
64.44	64.45			X			
65.90	65.91	X		X			
66.70	66.71			X			
68.59	68.60			X			
70.60	70.61						
71.27	71.28						
72.89	72.91						
73.61	73.62						
77.80	77.81						
81.98	81.99						
82.34	82.35						
101.03	101.04						
104.62	104.63		X				
107.37	107.38						
123.65	123.73						
127.11	127.12						
157.75	157.76						
190.81	190.82						
193.16	193.17						
195.58	195.59						

Given the high sediment accumulation rates in lower Oligocene sediments at the mouth of Mackay Valley (at Site CRP-3), the lowest occurrence of *R. antarctica* at 68.60 mbsf most likely represents a position well above the FO of this taxon. An age of *c.* 33.1 to 30.9 Ma is therefore inferred for the interval between *c.* 50 and 70 mbsf in CRP-3.

The FO of *Rhizosolenia oligocaenica* is inferred to be below the stratigraphic interval recovered in CRP-3, due to the presence of this well-dated diatom datum (*c.* 34 Ma from CIROS-1 drillcore and 33.3Ma in the Southern Ocean) below CRP-3 in the CIROS-1 drillcore (Fig. 2).

The section of CRP-3 below *c.* 70 mbsf is unzoned at the present time due to poor preservation. Moderately diverse, but poorly-preserved assemblages of siliceous microfossils, however, are noted sporadically down to *c.* 193 mbsf. In general, only the more robust and heavily-silicified forms, such as *Chaetoceros* spores, *Hemiaulus dissimilis*, *Pyxilla reticulata*, and *Stephanopyxis* spp., are preserved in this interval.

The absence of the heavily-silicified, hyaline remnants of *Hemiaulus characteristicus* in CRP-3 is notable, even in the poorly-preserved interval from *c.* 70 to 200 mbsf. The LO of this resistant and

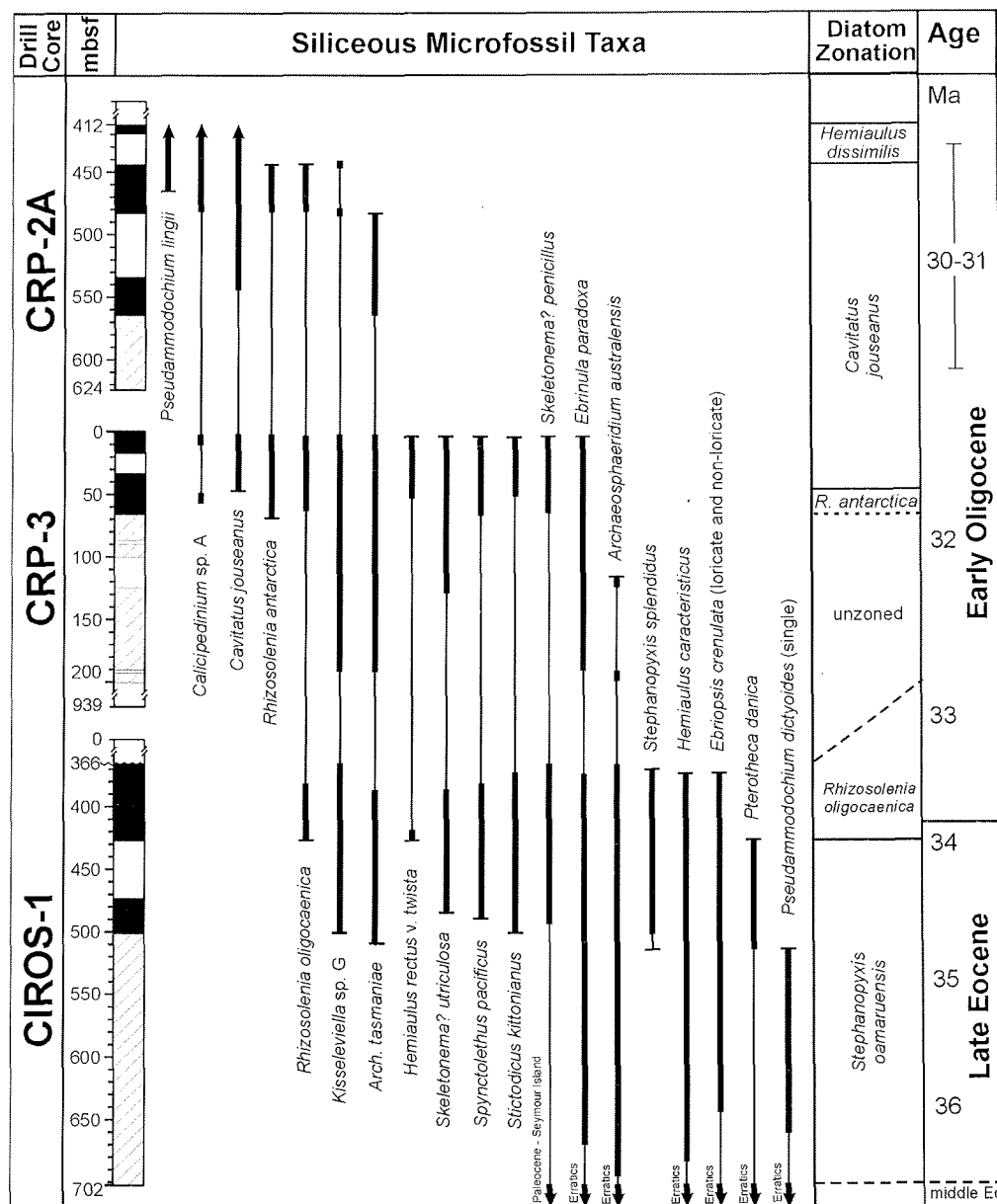


Fig. 2 - Comparison and correlation of the CRP-3 drillcore to higher stratigraphical intervals represented in the CRP-2/2A drillcore (Scherer et al., 2000), and lower intervals recovered in the CIROS-1 drillcore (Harwood, 1989) based on the biostratigraphical ranges of siliceous microfossil taxa. Number scale on left side of the figure represents metres below sea floor (mbsf) in the three drillcores. Intervals with diagonal lines represent barren intervals or intervals of extremely poor preservation of siliceous microfossils. Dark-grey boxes represent intervals containing abundant and well-preserved assemblages, and those shaded with light grey represent poorly-preserved assemblages. Thick vertical lines reflect the occurrence data for siliceous microfossil taxa in each of the drillholes. The thinner vertical lines reflect an interpretation of the composite range of these taxa between the drillcores.

distinctive diatom occurs within Subchron C13n in ODP Hole 744A (Baldauf & Barron, 1991). The LO of *H. characteristicus* is also known from DSDP Hole 511 within the lower part of the *Blackites spinosus* calcareous nannofossil Zone (see Fenner, 1984), but it occurs several 10s of meters below the FO of *Rhizosolenia antarctica* in DSDP Hole 511 (discussed above). From these data, the absence of *H. characteristicus* in CRP-3 supports an age assignment of younger than *c.* 33 Ma (Subchron C13n) for sediments above 200 mbsf.

#### OTHER AGE INFORMATION

The dominantly reversed polarity between 0 and 340 mbsf in CRP-3 is interpreted to represent a portion of Chron C12r. High sediment accumulation rates enabled the identification of numerous cryptochrons of normal polarity (Florindo et al., this volume). Below 340 mbsf, the magnetic polarity data are interpreted to represent Chrons C13n and C13r, with the Eocene-Oligocene boundary somewhere between 650 to 700 mbsf.

## CORRELATION TO OTHER DRILLCORES

Comparison of the diatom assemblages present near the bottom of CRP-2A with those in the upper intervals of CRP-3 provides a means to estimate the overlap of these two drillcores. However, the poor preservation and absence of siliceous microfossils in the lower 60 m of CRP-2A limits the resolution of this approach. Figure 2 presents the ranges of key siliceous microfossil taxa between these two drillcores. Note that 6 taxa present at the top of the CRP-3 drillcore do not continue into the lowest diatom-bearing intervals of CRP-2A at *c.* 564 mbsf. Taxa present in CRP-3, but not present in CRP-2A, include: *Hemiaulus rectus v. twisti*, *Skeletonema? utriculosa*, *Sphyncoletus pacificus*, *Stictodiscus? kittonianus*, *Skeletonema? penicillus* and *Ebrinula paradoxa*. *Kisseleviella sp. G* is common in CRP-3 samples, but occurs only rarely in 2 samples from CRP-2A. Additional evidence for the lack of a significant overlap between these drillcores comes from taxa in CRP-2A that do not occur, or are of limited range, in CRP-3. *Pseudammodochium lingii* occurs down to 465.00 mbsf in CRP-2A, but is absent in CRP-3. *Calicipedinium sp. A* occurs consistently down to 564.66 mbsf in CRP-2A, and only one questionable occurrence was noted at 7.86 mbsf in the CRP-3 drillcore. Siliceous microfossil assemblages in the upper portion of CRP-3 are sufficiently different from those in the lower portion of CRP-2A to argue for little to no overlap of these two drillcores.

The siliceous microfossil assemblages of CRP-3 are significantly different from the early Oligocene to late Eocene assemblages reported from the CIROS-1 drillcore (Harwood, 1989; Bohaty & Harwood, 2000). Several taxa present in the *Rhizosolenia oligocaenica* Zone, below the unconformity at *c.* 366 mbsf in CIROS-1 (Harwood et al., 1989a, Fig. 1), are absent from the diatom-bearing intervals of CRP-3. These taxa include the diatoms *Hemiaulus characteristicus*, *Stephanopyxis splendidus*, and *Pterotheca danica*, and the ebridians *Ebriopsis crenulata* (loricate and non-loriculate forms), *Parebriopsis fallax*, and *Pseudammodochium dictyoides*. This indicates that the upper *c.* 200 m of the CRP-3 drillcore is equivalent to part of the interval missing within the unconformity at *c.* 366 mbsf in CIROS-1.

A lowermost Oligocene diatom assemblage is also reported from ODP Hole 739C in Prydz Bay, Antarctica (Barron & Mahood, 1993; Mahood et al., 1993). This assemblage is interpreted to be equivalent to a portion of the *Rhizosolenia oligocaenica* Zone of Harwood et al. (1989a) from CIROS-1 and is calibrated to Subchrons C13n and C12r, within the calcareous nannofossil *Blackites spinosus* Zone (Barron & Mahood, 1993). Similar neritic diatom assemblages were recovered in CRP-3, but are slightly younger than those in the Prydz Bay section. This interpretation is based on the absence in CRP-3

of *Hemiaulus characteristicus*, *Pseudotriceratium adlerii*, and *Stephanopyxis splendidus*, all of which characterize the Prydz Bay assemblage.

Recent drilling in Prydz Bay during ODP Leg 188 also recovered a Palaeogene section containing well-preserved siliceous microfossils (Leg 188 Science Team, 2000). Assemblages present in Hole 1166A are similar to those in Hole 739C and below *c.* 366 mbsf in CIROS-1. Important diatom taxa common to the CIROS-1, 739C, and 1166A assemblages include *Kisseleviella sp. G*, *Hemiaulus characteristicus*, *Pterotheca danica*, and *Stephanopyxis splendidus*. However, the absence of several taxa in Hole 1166A, such as *Skeletonomopsis mahoodii* and *Sphyncoletus pacificus*, tentatively indicates that the 1166A section is slightly older than the diatom-bearing intervals of CRP-3, CIROS-1, and Hole 739C (Leg 188 Science Team, 2000).

## DIATOM PALAEOENVIRONMENTS

The combined presence of nannofossils and planktic marine diatoms in the upper *c.* 200 m of CRP-3 indicates normal marine conditions during deposition of these strata. Peak abundance of nannofossils is noted between *c.* 127 and 95 mbsf (Cape Roberts Science Team, 2000), and peak abundance of diatoms is noted between *c.* 64 and 35 mbsf. The abundant occurrence of diatoms or nannofossils in these intervals may reflect the influence of eutrophic vs. oligotrophic surface-water conditions, respectively (Cape Roberts Science Team, 2000). Poor preservation of biosiliceous material below *c.* 70 m, however, obscures the exact relationship between diatom and nannofossil occurrence.

Diatom assemblages recovered from CRP-3 are relatively uniform in composition and are dominated by marine neritic-planktic taxa of the genera *Chaetoceros*, *Stephanopyxis*, *Skeletonomopsis*, *Kisseleviella*, *Ikebea*, *Kannoa*, *Pseudotriceratium* and *Pyxilla* (Tab. 2). Benthic diatom taxa occur throughout this interval, but represent <5% of the total assemblage. Low abundance of benthic taxa and sporadic stratigraphical occurrence suggest displacement from an adjacent coastal-littoral zone into a depositional setting inferred to be below the euphotic zone. Based on these inferences, we interpret palaeo-water depths to be greater than 50-70 m. No significant changes in water depth were identified from the diatom assemblage data, and diatom genera associated with freshwater environments were not encountered in CRP-3.

Above *c.* 80 mbsf in CRP-3, several fluctuations in siliceous microfossil occurrence and abundance are noted, which are interpreted to reflect environmental changes. Low numbers of diatoms, and the poor state of preservation most likely reflects their ecological

exclusion due to a combination of influences high sediment input (turbidity), ice cover and low salinity. Generally, when sunlit, open marine conditions are present, diatoms will exploit this condition and deposition of diatom-rich sediment will result. Low numbers of diatoms, in conjunction with fragmented assemblages often indicate recycling and re-sedimentation of existing diatomaceous sediment.

Nearly all of the siliceous microfossil taxa present in CRP-3 are extinct. This precludes interpretation of palaeoenvironmental conditions based on the known distribution of modern taxa. The presence or absence of sea ice during sedimentation of the CRP-3 sequence is equivocal due to the unknown ecological affinities of Palaeogene taxa. Some diatom taxa have indirect (lineage) links to the modern sea ice environment. *Fragilariopsis* sp. A, for example, in the lower Miocene section of CRP-2/2A may indicate the presence of sea ice (Scherer et al., 2000). Similar taxa were not recognized in the CRP-3 drillcore.

### SUMMARY

The upper c. 70 m of CRP-3 contains abundant and well-preserved siliceous microfossil assemblages. Siliceous microfossils are present below this interval down to c. 200 mbsf, but are poorly preserved. All samples examined below 200 mbsf are barren. Well-preserved assemblages in the upper section are assigned a stratigraphical position of lower Oligocene, based on the presence of *Cavitatus jouseanus* (FO at 48.43 mbsf), *Rhizosolenia oligocaenica* (present from 3.05 to 63.64 mbsf), and *Rhizosolenia antarctica* (present from 3.05 to 68.59 mbsf). The FO of *Cavitatus jouseanus* is calibrated at c. 31 Ma from Southern Ocean cores, although it is rare and sporadic near its base. Additionally, the absence of *Hemiaulus characteristicus* in the upper 200 m of CRP-3 indicates an age younger than ~33 Ma, based on its calibrated LO from ODP Hole 744A.

Siliceous microfossil assemblages recovered in the CRP drillcores provide important new data toward the development of an Antarctic shelf biostratigraphy for the lower Miocene to middle lower Oligocene (CRP-2/2A) and the lower lower Oligocene (CRP-3). CRP drillcores span the interval from ~17 to 33 Ma, and provide a composite section to build a biostratigraphical framework based on siliceous microfossil datums. Calibration of zones and siliceous microfossil datums in CRP drillcores to the magnetic polarity time scale will considerably advance future age determinations of the Oligocene and lower Miocene on the Antarctic shelf.

New information on the stratigraphical distribution of siliceous microfossil assemblages from the Oligocene drillcores fills a stratigraphical gap that is present within the disconformity at c. 366 mbsf in the CIROS-1 drillcore. Collectively, the CIROS-1 (Harwood, 1989), CRP-1 (Harwood et al., 1998),

CRP-2/2A (Scherer et al., 2000) and CRP-3 (this report) drillcores document the history of Antarctic-neritic diatom evolution and southern high-latitude palaeobiogeography for the early Miocene to latest Eocene (c. 17 to 36 Ma).

### TAXONOMIC LIST AND RELEVANT SYSTEMATIC PALAEOONTOLOGY

The following is a listing of taxa or taxonomic groups encountered in this study. Many diatoms are reported only to genus level and many taxa are reported under informal names. Informal taxonomy presented here reflects the "work-in-progress" state of the Cape Roberts Project diatom studies. We do not include detailed reference to these taxa; the reader should refer to the works of Schrader & Fenner (1976), Fenner (1985), Harwood (1986), Harwood (1989), Harwood et al. (1989b), Harwood & Maruyama (1992), Barron & Mahood (1993), Mahood et al. (1993) for synonymy. Where necessary, we cross reference to species names used in the above papers, if names or taxonomic concepts have changed recently.

#### DIATOMS

*Actinopterychus senarius* (Ehrenberg) Ehrenberg.

*Actinopterychus splendens* (Shadbolot) Ralfs in Pritchard.

*Anaulus* sp.

*Arachnoidiscus* spp. Comments: Rare specimens of *Arachnoidiscus* spp. are present in CRP-3, which commonly occur as fragments.

*Asterolampra punctifera* (Grove) Hanna; Gombos & Ciesielski, 1983, p. 600, p. 431, pl. 2, figs. 4-8, pl. 5, figs. 8-10; Barron & Mahood, 1993, p. 38, pl. 4, fig. 13; Scherer et al., 2000, pl. 6, fig. 1.

*Asteromphalus oligocenicus* Schrader & Fenner; Gombos & Ciesielski, 1983, p. 600, pl. 5, figs. 5-7. (Pl. 5, Fig. 3)

*Aulacodiscus* spp.

*Biddulphia tuomeyi* (Bailey) Roper group; Harwood, 1989, p. 77, pl. 5, figs. 22-23.

*Biddulphia* sp. A of Harwood, 1989, p. 77, pl. 4, fig. 16.

*Cavitatus jouseanus* (Sheshukova) Williams; Akiba et al., 1993, p. 20-22, figs. 6-19, 6-20. Comments: Specimens of *Cavitatus jouseanus* present in CRP-3 differ from *C. jouseanus* s.s. in that they are smaller and more lightly silicified with narrow, tapered ends, rather than broadly-rounded ends. This morphology appears to be characteristic of "early forms" of *C. jouseanus*. (Pl. 1, Figs. 1-2)

*Cavitatus* sp. cf. *C. miocenicus* (Schrader) Akiba & Yanagisawa in Akiba. (Pl. 1, Fig. 3)

*Chaetoceros panduraeformis* (Pantocsek) Gombos; Scherer et al., 2000, p. 431, pl. 5, fig. 11.

*Chaetoceros* spp. and related spore-forming genera. Comments: Many distinct morphotypes of *Chaetoceros* are recognised, but are combined for this report. **Group A** includes simple Hyalochæte spores and vegetative cells of the variety abundant in modern Antarctic sediments (see Harwood, 1986, pl. 7, figs. 1-12). **Group B** includes larger spores with



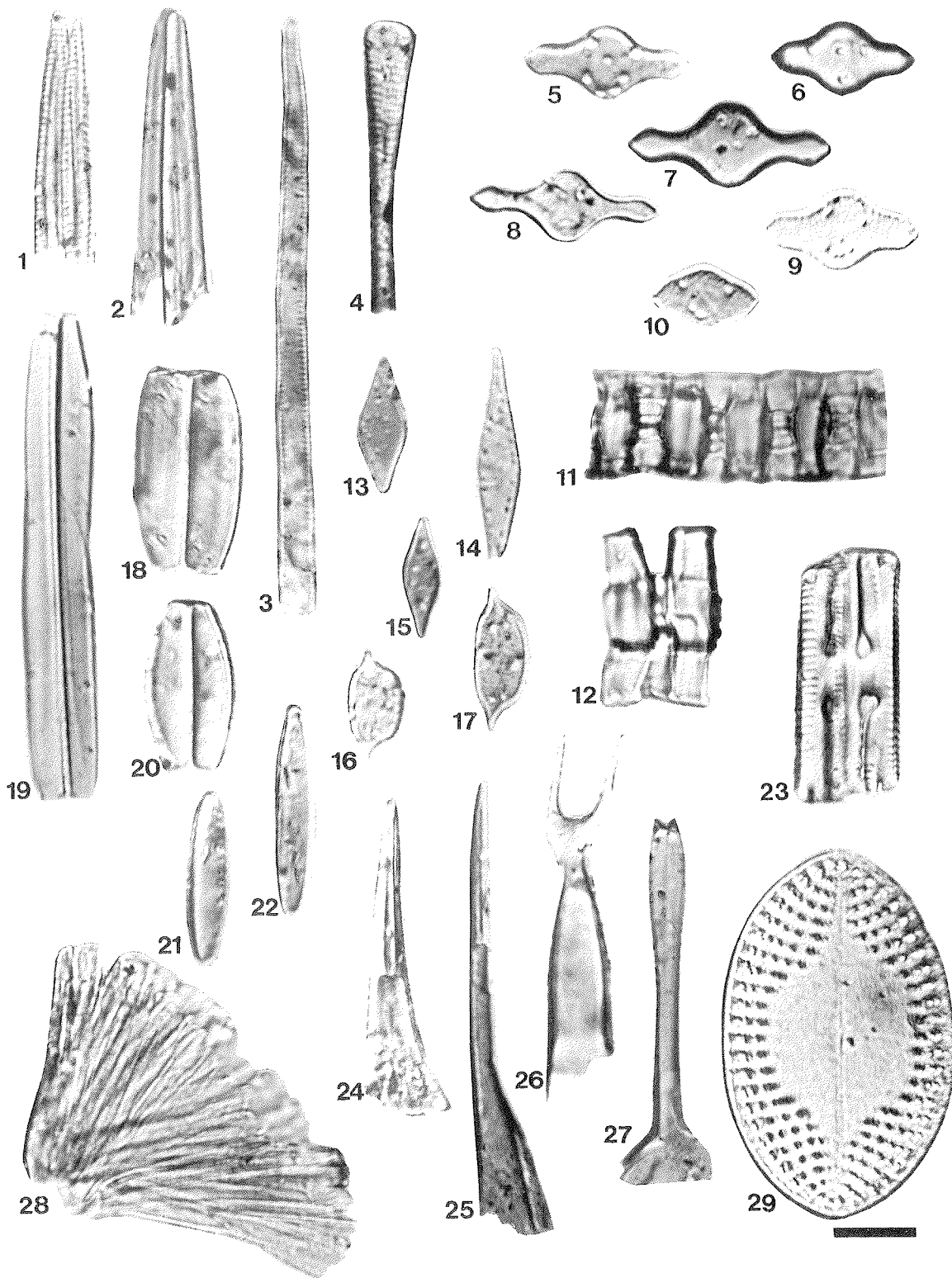


Plate 1 - Scale bar equals 10  $\mu$ m. All figures are valve views unless indicated otherwise.

Figures 1-2. *Cavitatus jouseanus* (Sheshukova) Williams - "early form"; (1) CRP3-44.93-.99 mbsf; (2) CRP3-48.43-.44 mbsf. Figure 3. *Cavitatus* sp. cf. *C. miocenicus* (Schrader) Akiba & Yanagisawa; CRP3-38.78-.79 mbsf. Figure 4. *Sceptroneis talwanii* Schrader & Fenner; CRP3-9.69-.70 mbsf. Figures 5-12. *Kisseleviella* sp. G of Scherer et al. (2000); (5) CRP3-37.29-.30 mbsf; (6) CRP3-12.19-.20 mbsf; (7) CRP3-28.44-.45 mbsf; (8) CRP3-10.78-.79 mbsf; (9) CRP3-12.19-.20 mbsf; (10) CRP3-10.78-.79 mbsf; (11) Girdle view, CRP3-54.77-.78 mbsf; (12) Girdle view, CRP3-54.19-.20 mbsf. Figures 13, 15. *Kisseleviella* sp. D of Scherer et al. (2000); (13) CRP3-43.70-.71 mbsf; (15) CRP3-3.05-.06 mbsf. Figure 14. *Kisseleviella*?/*Cymatosira*? sp., CRP3-3.05-.06 mbsf. Figures 16-17. *Kisseleviella* sp. F of Scherer et al. (2000); (16) CRP3-33.95-.96 mbsf; (17) CRP3-28.70-.71 mbsf. Figures 18-22. *Ikebea* sp. D; (18) Girdle view, CRP3-5.47-.48 mbsf; (19) Girdle view, CRP3-12.19-.20 mbsf; (20) Girdle view, CRP3-7.85-.86 mbsf; (21) CRP3-33.95-.96 mbsf; (22) CRP3-28.70-.71 mbsf. Figure 23. *Grammatophora marina* (Lyngbye) Kützing; Girdle view, CRP3-57.71-.72 mbsf. Figure 24. *Rhizosolenia oligocaenica* Schrader; CRP3-5.47-.48 mbsf. Figure 25. *Rhizosolenia* sp.; CRP3-3.05-.06 mbsf. Figure 26. *Pseudopyxilla americana* (Ehrenberg) Forti; CRP3-28.70-.71 mbsf. Figure 27. Genus et sp. indet.; CRP3-48.43-.44 mbsf. Figure 28. *Ikebea* sp. B of Scherer et al. (2000); Colony, CRP3-12.19-.20 mbsf. Figure 29. *Cocconeis* sp.; CRP3-44.18-.27 mbsf.

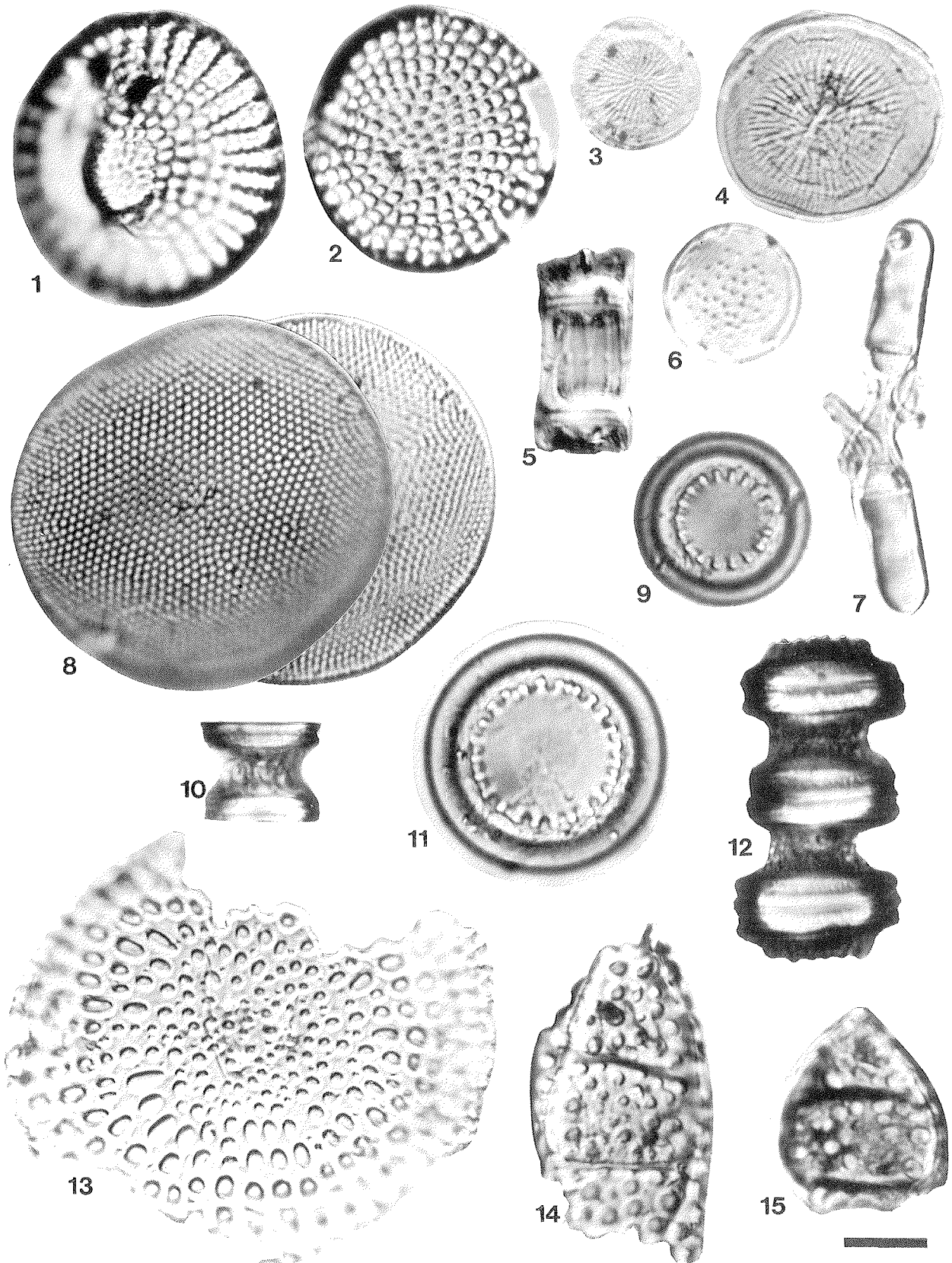


Plate 2 - Scale bar equals 10  $\mu$ m. All figures are valve views unless indicated otherwise.

Figures 1-2. *Stictodiscus? kittonianus* Greville; (1) CRP3-7.85-.86 mbsf; (2) CRP3-49.67-.68 mbsf. Figures 3-4. *Thalassiosira? mediaconvexa* Schrader & Fenner; (3) CRP3-44.93-.94 mbsf; (4) CRP3-54.19-.20 mbsf. Figures 5-6. *Skeletonomopsis mahoodii* Sims; (5) Girdle view, CRP3-55.77-.78 mbsf; (6) CRP3-57.71-.72 mbsf. Figure 7. *Skeletonema? penicillus* Grunow in Van Heurck; Two specimens in girdle view, CRP3-33.95-.96 mbsf. Figure 8. *Stellarima microtrias* Hasle & Sims; High/low focus, CRP3-10.78-.79 mbsf (note presence of only two central labiate processes). Figures 9-12. *Skeletonema? utriculosa* Brun; (9) CRP3-5.47-.48 mbsf; (10) Girdle view, CRP3-49.67-.68 mbsf; (11) CRP3-10.78-.79 mbsf; (12) Girdle view, CRP3-37.29-.30 mbsf. Figure 13. *Sphinctoletthus pacificus* (Hajós) Sims; CRP3-7.85-.86 mbsf. Figures 14-15. *Sphinctoletthus* sp. A; CRP3-54.19-.20 mbsf.

- large bifurcate setae such as illustrated by Harwood, 1986, pl. 3, figs. 1-4; Harwood et al., 1989b, Pl. 3, Fig. 4. **Group C** is an informal grouping of numerous relatively large and heavily-silicified spore "genera," including *Chaetoceros*-like resting-spores referred to as *Chasea* Hanna and *Xanthiopyxis* Ehrenberg, among others. (Pl. 5, Figs. 6, 8, 12, 13)
- Chaetoceros* sp. of Harwood, 1986, pl. 7, fig. 1.
- Chaetoceros* resting spore A of Barron & Mahood, 1993, p. 44, pl. 5, figs. 13, 16.
- Cocconeis* spp. (Pl. 1, Fig. 29).
- Coscinodiscus* spp. Comments: This group includes many large *Coscinodiscus* species, which are generally present as fragments in unsieved samples.
- Diploneis* spp.
- Eurossia irregularis* var. *irregularis* (Greville) Sims in Mahood et al., 1993, p. 254-255; Scherer et al., 2000, p. 434, pl. 4, figs. 1, 2, 7, 9; *Triceratium hebetatum* (Grunow) sensu Harwood, 1989; *Triceratium polymorphum* Harwood & Maruyama 1992, pro parte. Comments: We observed heterovalvy on some frustules of this taxon (Pl. 3, Figs. 1-3). One valve displays the normal characteristics of *Eurossia irregularis* var. *irregularis*. The other valve morphotype, however, is thick-walled with a raised, swollen valve center; the areolae on this morphology are small, 5 – 6 in 10  $\mu\text{m}$ , and inter-areolar architecture is thick with an echinate texture. Distinguishing processes at the apices of the centrally-swollen valve were not observed in LM examination. Neither resting spores nor heterovalvy have been previously reported for this genus. (Pl. 3, Figs. 1-8)
- Goniothecium decoratum* Brun; Schrader & Fenner, 1976, p. 982, pl. 6, figs. 3, 5; pl. 37, figs. 1-5, 11-14. (Pl. 3, Figs. 11-12)
- Goniothecium odontella* Ehrenberg. (Pl. 3, Fig. 10)
- Grammatophora marina* (Lyngbye) Kützing. (Pl. 1, fig. 23)
- Grammatophora* sp.; Scherer et al., 2000, pl. 2, fig. 20.
- Hemiaulus dissimilis* Grove & Sturt; Scherer et al., 2000, p. 434, pl. 3, figs. 12-13; Harwood & Bohaty, 2000, p. 92, pl. 5, fig. t. Note: This taxon could be better placed in the genus *Ailuretta* (see Sims, 1986). (Pl. 6, Figs. 5-8).
- Hemiaulus incisus* Hajós. Comments: One specimen of this taxon was encountered at 38.78 mbsf.
- Hemiaulus* sp. cf *H. mitra* Grunow.
- Hemiaulus polycystinorum* Ehrenberg. Scherer et al., 2000, p. 434, pl. 3, fig. 17.
- Hemiaulus rectus* var. *twista* Fenner, 1984, p. 332, pl. 2, fig. 6. (Pl. 6, Figs. 9-10)
- Hemiaulus* sp. B of Scherer et al., 2000, p. 434, pl. 3, fig. 16. (Pl. 6, Fig. 3)
- Hemiaulus* sp. D. Description: This morphology possesses one "tapered" arm and one "boxy" arm. Some specimens are slightly curved in girdle view. (Pl. 6, Figs. 1-2, 4)
- Ikebea* sp. A of Scherer et al., 2000, pl. 1, fig. 25. Comments: This form is small, lightly-silicified, and narrow in transapical width. Striae and marginal spines were not identified in LM observations.
- Ikebea* sp. B of Scherer et al., 2000, p. 434, pl. 1, figs. 22-23. Comments: This form is larger than *Ikebea* sp. A; striae and marginal spines were not visible in LM observations. (Pl. 1, Figs. 28)
- Ikebea* sp. D; Genus et sp. indet. D of Harwood, 1989, pl. 4, p. 82, figs. 26-28. Description: This form is hyaline and rounded in girdle view. Considerable variability in length is noted (compare fig. 19 and fig. 21 on pl. 1). Specimens were commonly observed in girdle view paired with another valve (see pl. 1, figs. 18-20). Marginal spines were observed on some specimens. (Pl. 1, Figs. 18-22; Pl. 9, Fig. 4)
- Isthmia* spp. Comments: Fragments of *Isthmia* spp. occur throughout the diatom-bearing interval of CRP-3.
- Kanuoia hastata* Komura, 1980, p. 376, text-fig. 3, pl. 46, figs. 13a-b; Scherer et al., 2000, p. 434, pl. 1, figs. 26-27; *Ikebea tenuis* (Brun) Akiba of Harwood, 1989, p. 79, pl. 4, fig. 34.
- Genus *Kisseleviella* Sheshukova. Comments: Several diatom taxa observed in CRP-3 samples are assigned to the genus *Kisseleviella*. Informal designation for these forms follow from those applied in the CRP-2/2A report; see Scherer et al. (2000, p. 434, 436) for additional comments.
- Kisseleviella* sp. C of Scherer et al., 2000, p. 436, pl. 1, figs. 8-13. Description: Valve 20 to 40  $\mu\text{m}$  in length with maximum width of ~6  $\mu\text{m}$ , covered by faint pores; valve is inflated-lanceolate in shape with protracted, rounded apices. The central array of linking spines is arranged in a disorganized fashion. Location of secondary or lateral linking structures is not obvious and when present represented by single elements.
- Kisseleviella* sp. D. of Scherer et al., 2000, p. 436, pl. 1, figs. 14-17. Description: Valve 10 to 15  $\mu\text{m}$  in length with a maximum width of ~6  $\mu\text{m}$ ; valve is lanceolate in shape with very slightly protracted apices. Many specimens also show a slight bilateral asymmetry with "rotated" apices. 3 to 10 linking spines are commonly present arranged in a single, central ring or disorganized fashion. *Kisseleviella* sp. C and *Kisseleviella* sp. D may represent different size cells of the same taxon. (Pl. 1, Figs. 13, 15)
- Kisseleviella* sp. F of Scherer et al., 2000, p. 436, pl. 1, fig. 19; Resting spore B of Barron & Mahood, 1993, p. 44, pl. 5, figs. 17, 19. Description: Valve is linear-lanceolate and bilaterally assymetrical in shape with sharply tapered (or apiculated) apices, ~25  $\mu\text{m}$  in length with a maximum width of ~8  $\mu\text{m}$ . (Pl. 1, Figs. 16-17)
- Kisseleviella* sp. G of Scherer et al., 2000, p. 436, pl. 1, figs. 20-21; *Kisseleviella carina* sensu Harwood, 1989 (in part), p. 79, pl. 4, fig. 37, not figs. 35, 36. Description: Valve shape is inflated-lanceolate with apiculated, sub-capitate apices, 20 to 30  $\mu\text{m}$  in length with a maximum width of ~12  $\mu\text{m}$ ; 5 to 10 central linking spines are arranged in a single, offset ring, or in a random distribution. Secondary or lateral linking spines consist of a single "post-and-crown" (or spiny and annular tubercle) structure, and are bilaterally offset. (Pl. 1, Figs. 5-12)
- Kisseleviella* sp. H. Remarks: This diatom is morphologically similar to *Kisseleviella* sp. G, but differs in possessing a greater inflation of the sub-capitate apices to nearly the width of the central inflated area, and the apices are mucronate.
- Kisseleviella?* sp. / *Cymatosira?* sp. (Pl. 1, Fig. 14).

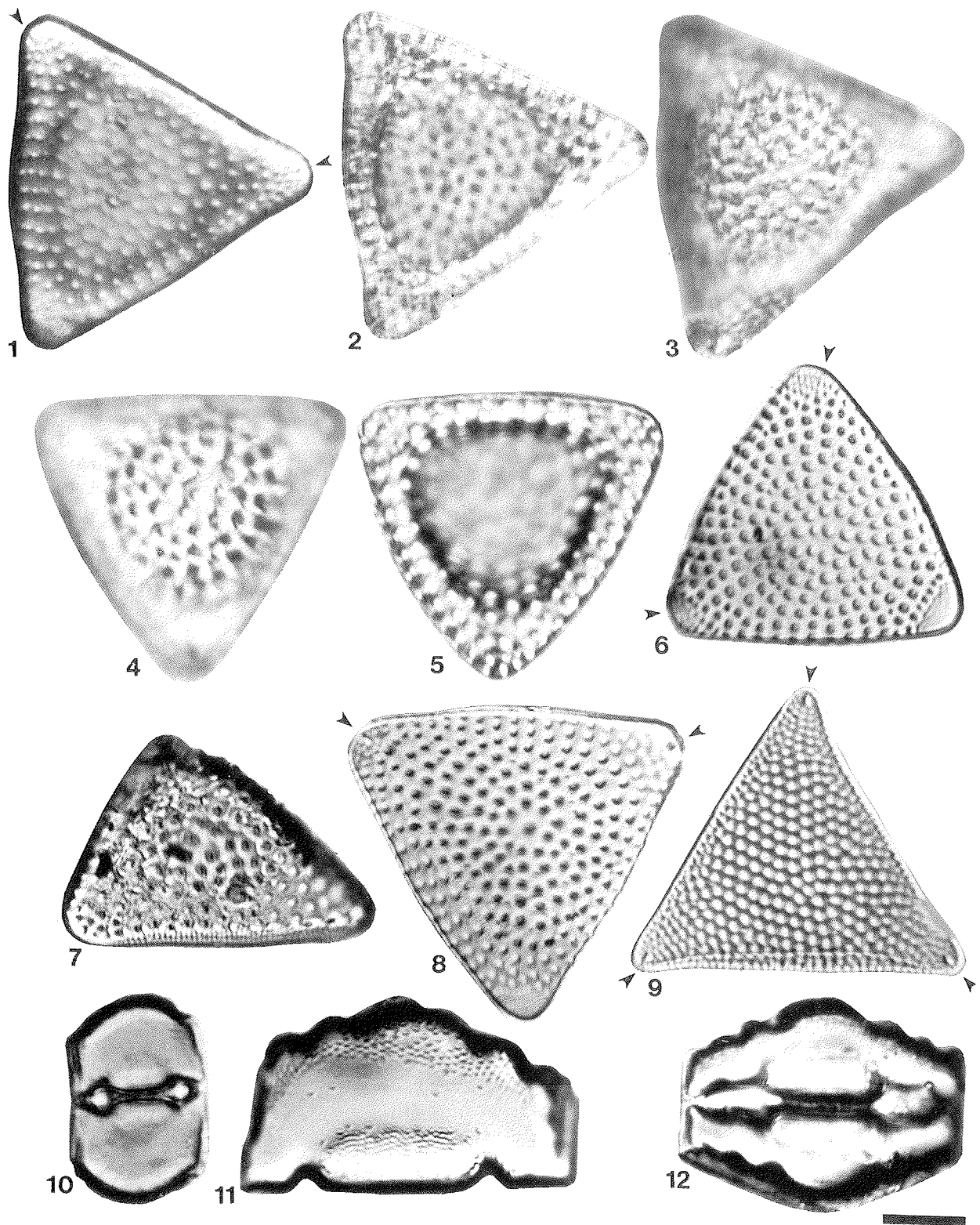


Plate 3 - Scale bar equals 10  $\mu$ m. All figures are valve views unless indicated otherwise. Arrows denote positions of labiate processes. Figures 1-8. *Eurossia irregularis* var. *irregularis* (Greville) Sims; (1-3) Complete hetero- valve frustle, low/middle/high focus of the same specimen, CRP3-54.77-.78 mbsf; (4-5) Centrally-swollen hypo- valve, high/low focus of the same specimen, CRP3-49.67-.68 mbsf; (6) CRP3-28.70-.71 mbsf; (7) Centrally-swollen hypo- valve, oblique view, CRP3-54.19-.20 mbsf; (8) CRP3-7.85-.86 mbsf. Figure 9. *Pseudotriceratium radiosoreticulatum* (Grunow in Van Heurck) Fenner; (9) CRP3-57.71-.72 mbsf. Figures 10. *Goniothecium odontella* Ehrenberg; Girdle view, CRP3-10.78-.79 mbsf. Figures 11, 12. *Goniothecium decoratum* Brun; (11) Girdle view, CRP3-28.70-.71 mbsf; (12) Girdle view, CRP3-49.67-.68 mbsf.

- Liradiscus ovalis* Greville; Hajós, 1976, p. 826, pl. 17, figs. 1, 2; Harwood & Bohaty, 2000, p. 95, pl. 9, figs. t, u.
- Navicula?* spp. Comments: Small, lightly-silicified forms possibly belonging to the genus *Navicula* were observed in several CRP-3 samples.
- Odontella fimbriata* (Greville) Schrader in Schrader & Fenner; Barron & Mahood, 1993, p. 40, pl. 4, figs. 6a, b.
- Paralia sol* var. *marginalis* (Peragallo) Harwood, 1989, p. 79, pl. 5, fig. 12. (Pl. 5, Fig. 14)
- Paralia sulcata* (Ehrenberg) Cleve.
- Psammodiscus* Round & Mann sp.
- Pseudopyxilla americana* (Ehrenberg) Forti. (Pl. 1, Fig. 26)
- Pseudotriceratium radiosoreticulatum* (Grunow in Van Heurck) Fenner; Barron & Mahood, 1993, p. 42, pl. 3, fig. 5; Mahood et al., 1993, p. 259, figs. 45-48, 72; Scherer et al., 2000, p. 436, pl. 4, fig. 3. (Pl. 3, Fig. 9)
- Pterotheca?* sp. A; Scherer et al., 2000, p. 436, pl. 6, fig. 6; *Pterotheca* sp. of Schrader & Fenner, 1976, pl. 43, fig. 14. Remarks: Compare this diatom with *Rhizosolenia* sp. C of Harwood, 1989, p. 80, pl. 3, fig. 25.
- Pterotheca* sp. B of Harwood, 1989, p. 80, pl. 3, fig. 18.
- Pterotheca* sp. C of Harwood, 1989, p. 80, pl. 3, fig. 20.
- Pterotheca* sp. D of Harwood, 1989, p. 80, pl. 5, figs. 16-17.
- Pyrgopyxis eocena* Hendy; Scherer et al., 2000, p. 436, pl. 5, fig. 9. Remarks: Compare with Miocene diatom *Biturricula unca* Komura 1999, p. 22, 25, figs. 11-13, 96-112, text figure 2 and *Pyxilla* spp. (Pl. 4, Fig. 5)
- Pyxilla johnsoniana* Greville. (Pl. 4, Figs. 2, 6-8, 10)
- Pyxilla reticulata* Grove & Sturt; Harwood, 1989, p. 80, pl. 3, figs. 7-10; Barron & Mahood, 1993, p. 42, pl. 7, figs. 1-3. (Pl. 4, Figs 1, 3, 4, 9)
- Radialiplicata clavigera* (Grunow in Van Heurck) Gleser. (Pl. 5, Figs. 1-2)
- Rhabdonema japonicum* Tempère & Brun group.
- Rhabdonema* sp. cf. *R. elegans* Tempère & Brun; Harwood, 1989, p. 80; Scherer et al., 2000, p. 436, pl. 5, fig. 12; Gen et sp. uncertain 1 of Harwood, 1986, p. 87, pl. 5, figs. 11-12.
- Rhabdonema* sp. A of Harwood, 1989, p. 80, pl. 6, figs. 7-8. Comments: This form is present in one sample at 48.18 mbsf.
- Rhabdonema* spp. /*Grammatophopra* spp. Comments: Specimens of several unknown *Grammatophora* spp. and *Rhabdonema* spp. are present in many CRP-3 samples (see Scherer et al., 2000, pl. 2, figs. 17, 20, for illustrated examples).
- Rhizosolenia antarctica* Fenner, 1984, p. 333, pl. 2, fig. 5; Scherer et al., 2000, pl. 3, figs. 1-2.
- Rhizosolenia hebetata* Bailey group; Scherer et al., 2000, pl. 3, figs. 6-7.
- Rhizosolenia oligoceanica* Schrader, 1976, p. 635, pl. 9, fig. 7; Barron & Mahood, 1993, p. 42, pl. 5, figs. 1-2; Scherer et al., 2000, p. 436, pl. 3, figs. 3-4. (Pl. 1, Fig. 24)
- Rhizosolenia* sp. A of Harwood, 1989, p. 80, pl. 3, fig. 26.
- Rhizosolenia* sp. B of Harwood, 1989, p. 80, pl. 3, fig. 27.
- Rhizosolenia* sp. C of Harwood, 1989, p. 80, pl. 3, fig. 25. Remarks: compare with *Pterotheca* sp. A of Scherer et al., 2000, p. 436, pl. 6, fig. 6.
- Rhizosolenia* sp. (Pl. 1, Fig. 25)
- Rocella praenitida* (Fenner) Fenner ex Kim & Barron; Scherer et al., 2000, p. 436, pl. 5, fig. 2. (Pl. 5, Figs. 4-5)
- Rouxia granda* Schrader in Schrader & Fenner, p. 997, pl. 7, fig. 17; Harwood, 1989, p. 80; Barron & Mahood, 1993, p. 42, pl. 4, figs. 2-3.
- Sceptroneis lingulatus* Fenner; Gombos & Ciesielski, 1983, pl. 24, fig. 8; Harwood, 1989, p. 80, pl. 6, fig. 11; Barron & Mahood, 1993, p. 42, pl. 5, fig. 10.
- Sceptroneis propinqua* Schrader & Fenner; Scherer & Koç, 1996, pl. 2, fig. 6.
- Sceptroneis talwanii* Schrader & Fenner, 1976, pl. 24, figs. 28-29; Barron & Mahood, 1993, p. 42, pl. 5, fig. 9, pl. 7, figs. 4a,b. (Pl. 1, Fig. 4)
- Skeletonema?* *penicillus* Grunow in Van Heurck; Harwood, 1989, p. 80, pl. 5, figs. 14-15; Sims, 1994, p. 402-405, figs. 37-40, 53; *Corethron penicillus* (Grunow) Fenner, 1994, p. 109, pl. 4, fig. 4. (Pl. 2, Fig. 7)
- Skeletonema?* *utriculosa* Brun; Sims, 1994, p. 402, figs. 33-36, 51-52. Comments: This taxon should be transferred out of *Skeletonema* and placed within or near the recently proposed genus *Trochosirella* Komura, 1996, p. 9-10. Komura (1996) distinguishes this taxon from *Trochosirella* by the "type of areolae, the exit morphology of the rimoportules and the architecture in the greater part of the valve face." Some specimens that lack the ring of lingulate elevations are interpreted to be separation valves. (Pl. 2, Figs. 9-12)
- Skeletonemopsis mahoodii* Sims, 1994, p. 397-402, figs. 25-32, 48; Scherer et al., 2000, p. 440, pl. 2, figs. 8-12; *Skeletonemopsis barbadensis* sensu Barron & Mahood, 1993, p.42, pl. 6, fig. 1. (Pl. 2, Figs. 5-6; Pl. 9, Fig. 6)
- Sphinctoletus hemiauloides* Sims, 1986, p. 246, figs. 16-22, 64-65.
- Sphinctoletus pacificus* (Hajós) Sims, 1986, p. 250, figs. 29-34, 69; Harwood, 1989, p. 80, pl. 4, fig. 8. (Pl. 2, Fig. 13)
- Sphinctoletus* sp. A. (Pl. 2, Figs. 14-15)
- Stellarima microtrias* Hasle & Sims. (Pl. 2, Fig. 8)
- Stellarima primalabiata* (Gombos) Hasle and Sims.
- Stellarima stellaris* (Roper) Hasle & Sims.
- Stephanopyxis megapora* Grunow.
- Stephanopyxis oamaruensis* Hajós, 1976, p. 825, pl. 19, figs. 5-8; Harwood, 1989, p. 81, pl. 2, figs. 27-29; Barron & Mahood, 1993, p. 42, pl. 2, fig. 5; Scherer et al., 2000, p. 440, pl. 5, fig. 7. Remarks: SEM examination will likely indicate that this taxon should be transferred to genus *Stephanonycites*, and perhaps be conspecific with *Stephanonycites variegates* Komura 1999, p. 33-37, text-figure 4, figs 20-22, 46, 164-195.
- Stephanopyxis spinosissima* Grunow; Schrader & Fenner, 1976, p. 1000, pl. 31, fig. 5; Harwood, 1989, p. 81; *Stephanopyxis* sp. A of Harwood, 1986, p. 87, pl. 4, fig. 2.
- Stephanopyxis superba* (Greville) Grunow; Harwood, 1989, p. 81, pl. 2, figs. 14-20, 26.
- Stephanopyxis* sp. cf. *S. superba* (Greville) Grunow. (Pl. 7, Figs. 7-8; Pl. 9, Fig. 3)

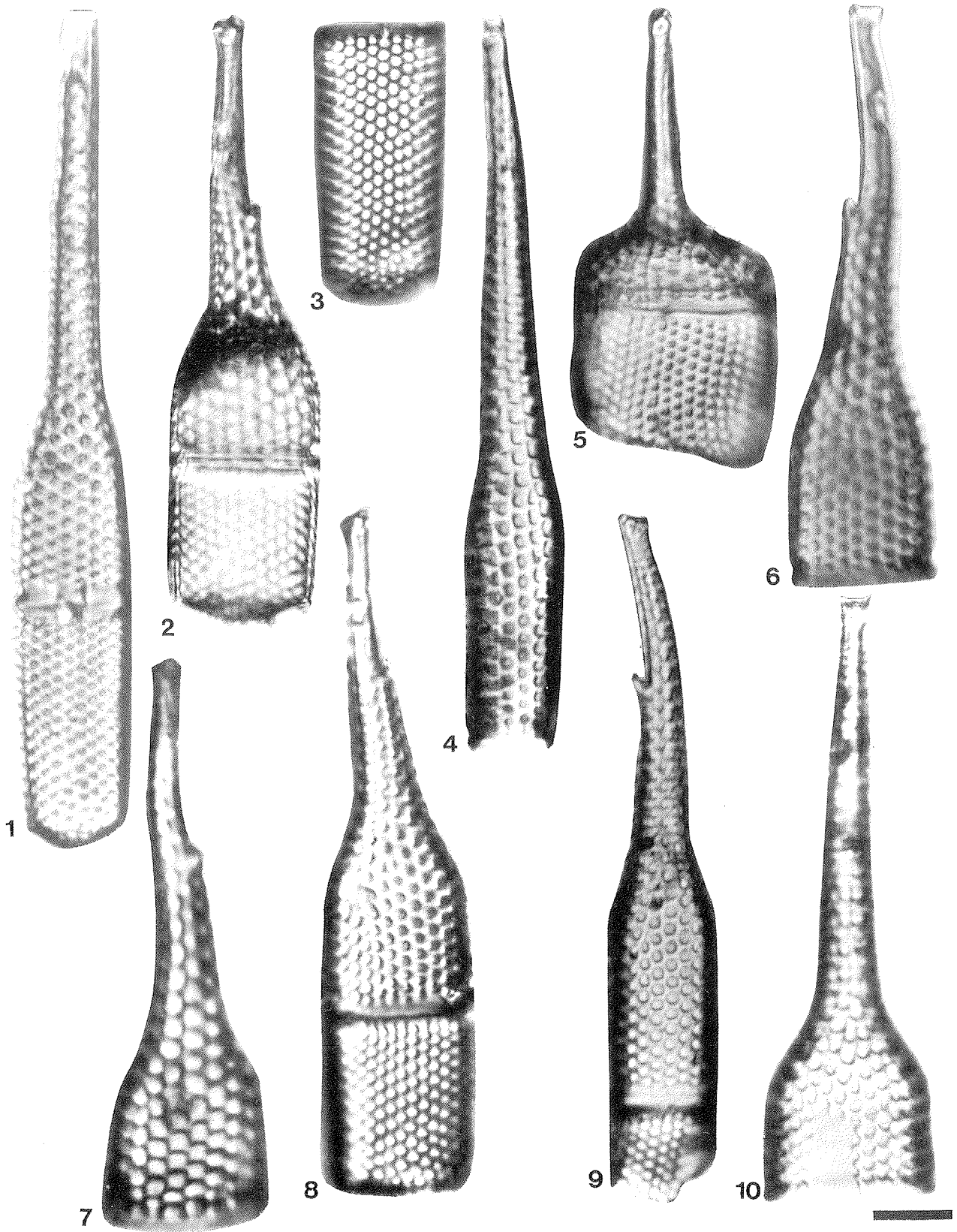


Plate 4 - Scale bar equals 10  $\mu$ m.

Figures 1, 3, 4, 9. *Pyxilla reticulata* Grove & Sturt; (1) CRP3-10.78-.79 mbsf; (3) CRP3-54.19-.20 mbsf; (4, 9) CRP3-7.85-.86 mbsf.  
 Figures 2, 6, 7, 8, 10. *Pyxilla johnsoniana* Greville; (2, 8) CRP3-54.19-.20 mbsf; (6) CRP3-5.01-.02 mbsf; (7, 10) CRP3-49.67-.68 mbsf.  
 Figure 5. *Pygrupyxis eocena* (Hendy); (5) CRP3-7.85-.86 mbsf.

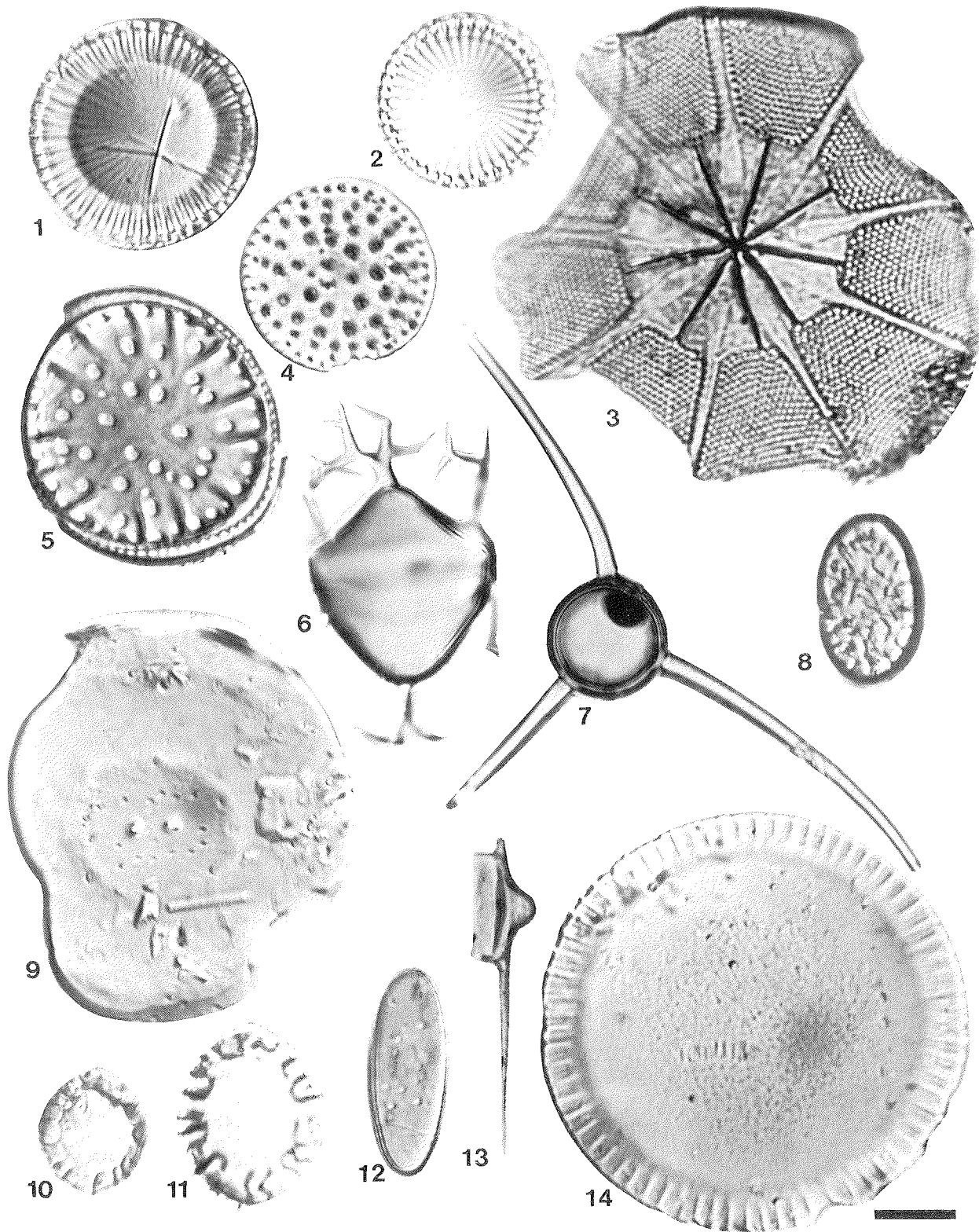


Plate 5 - Scale bar equals 10  $\mu$ m. All figures are valve views unless indicated otherwise.

Figures 1-2. *Radialiplicata clavigera* (Grunow in Van Heurck) Gleser; (1) CRP3-33.95-.96 mbsf; (2) CRP3-28.70-.71 mbsf. Figure 3. *Asteromphalus oligocenicus* Schrader & Fenner; CRP3-37.29-.30 mbsf. Figures 4, 5. *Rocella praeinitida* (Fenner) Fenner ex Kim & Barron; (4) CRP3-10.78-.79 mbsf; (5) CRP3-54.19-.20 mbsf. Figures 6, 8, 12, 13. *Chaetoceros* spp.; (6, 12) CRP3-28.70-.71 mbsf; (8) CRP3-49.67-.68 mbsf; (13) CRP3-48.43-.44 mbsf. Figures 10-11. Genus et sp. indet. C of Harwood (1989); (10) CRP3-44.93-.94 mbsf; (11) CRP3-33.95-.96 mbsf. Figure 7. *Archaeosphaeridium tasmaniae* Perch-Nielsen (chrysothrix cyst); CRP3-50.47-.48 mbsf. Figure 9. *Vulcanella hanna* Sims & Mahood; CRP3-5.47-.48 mbsf. Figure 14. *Paralia sol* var. *marginalis* (Peragallo) Harwood; CRP3-7.85-.86 mbsf.

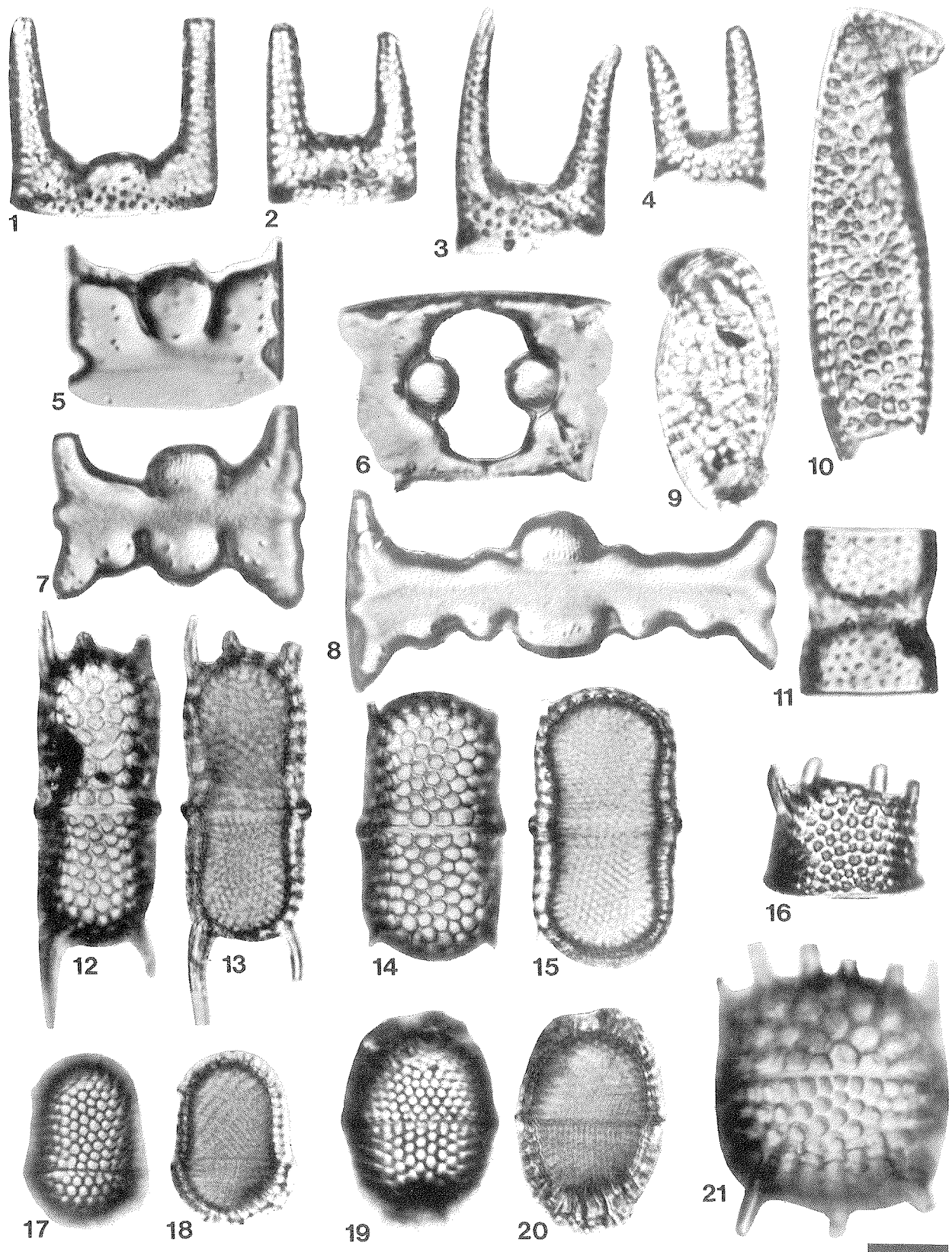


Plate 6 - Scale bar equals 10  $\mu$ m. All figures girdle view except figs. 9-10.

Figures 1-2, 4. *Hemiaulus* sp. D (1) CRP3-44.18-.27 mbsf; (2) CRP3-54.19-.20 mbsf; (4) CRP3-49.67-.68 mbsf. Figure 3. *Hemiaulus* sp. B of Scherer et al. (2000); (3) CRP3-7.85-.86 mbsf. Figures 5-8. *Hemiaulus dissimilis* Grove & Sturt; (5) CRP3-28.70-.71 mbsf; (6) CRP3-5.01-.02 mbsf; (7) CRP3-5.47-.48 mbsf; (8) CRP3-10.78-.79 mbsf. Figures 9-10. *Hemiaulus rectus* var. *twista* Fenner; (9) CRP3-54.19-.20 mbsf; (10) CRP3-33.95-.96 mbsf. Figure 11. *Stephanopyxis* sp. 7; CRP3-55.77-.78 mbsf. Figures 12-15. *Stephanopyxis turris* (Greville & Arnott) Ralfs in Pritchard; (12-13) High/low focus, CRP3-54.19-.20 mbsf; (14-15) High/low focus of the same specimen, CRP3-54.19-.20 mbsf. Figure 16, 21. *Stephanopyxis* sp. 2; (16) CRP3-57.71-.72 mbsf; (21) CRP3-57.71-.72 mbsf. Figures 17-18. *Stephanopyxis* sp. 9; (17-18) High/low focus of the same specimen, CRP3-54.19-.20 mbsf. Figures 19-20. *Stephanopyxis* sp. 4; (19-20) High/low focus of the same specimen, CRP3-37.29-.30 mbsf.



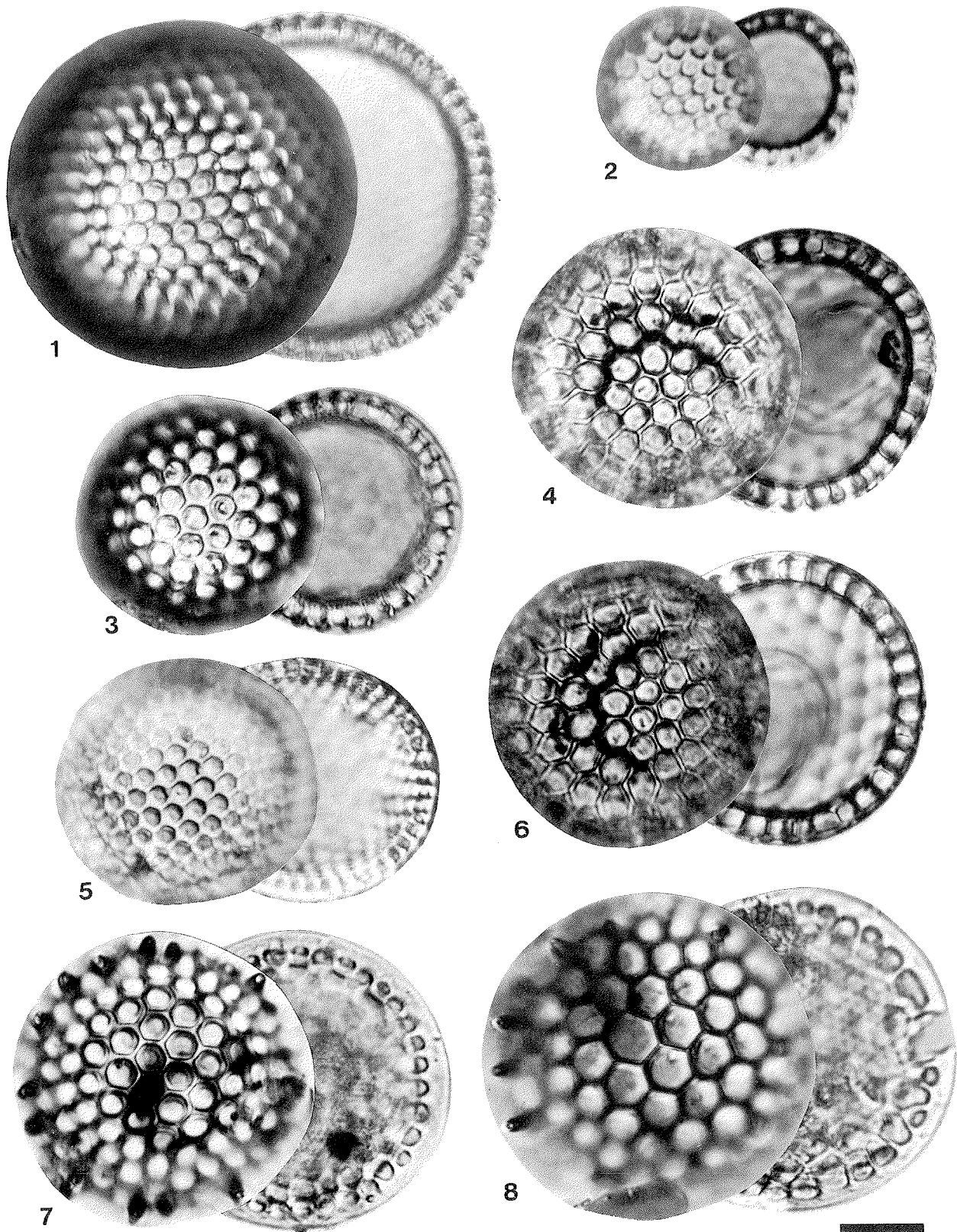


Plate 7 - Scale bar equals 10  $\mu$ m. All figures are valve views.

Figure 1. *Stephanopyxis* sp. 5; High/low focus of the same specimen, CRP3-54.19-.20 mbsf (note presence of two central processes). Figure 2. *Stephanopyxis* sp.; (2) High/low focus of the same specimen, CRP3-54.19-.20 mbsf. Figures 3, 5. *Stephanopyxis* sp. 8; (3) High/low focus of the same specimen, CRP3-54.19-.20 mbsf; (5) High/low focus of the same specimen, CRP3-54.19-.20 mbsf. Figures 4, 6. *Stephanopyxis* sp. 3; (4) High/low focus, CRP3-54.19-.20 mbsf; (6) High/low focus of the same specimen, CRP3-54.19-.20 mbsf. Figures 7-8. *Stephanopyxis* sp. cf. *S. superba* (Greville) Grunow (7) High/low focus of the same specimen, CRP3-54.19-.20 mbsf; (8) High/low focus of the same specimen, CRP3-54.19-.20 mbsf.

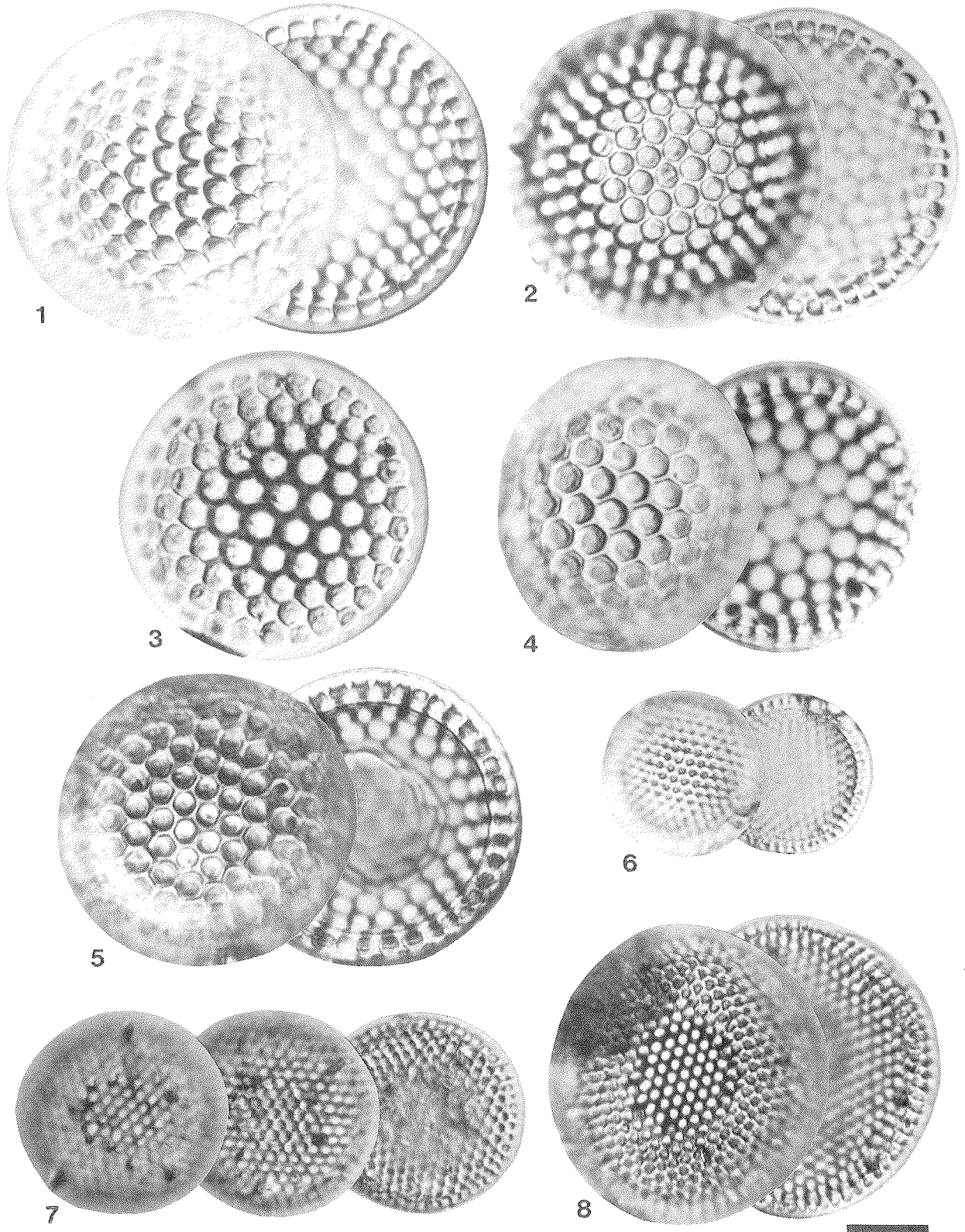


Plate 8 - Scale bar equals 10  $\mu$ m. All figures are valve views.

Figures 1-4. *Stephanopyxis* sp. 1; (1) High/low focus of the same specimen, CRP3-28.70-.71 mbsf; (2) High/low focus of the same specimen, CRP3-37.29-.30 mbsf; (3) High/low focus of the same specimen, CRP3-12.19-.20 mbsf; (4) High/low focus of the same specimen, CRP3-57.71-.72 mbsf. Figure 5. *Stephanopyxis* sp. 3; High/low focus of the same specimen, CRP3-54.19-.20 mbsf. Figure 6. *Stephanopyxis* sp. 10; High/low focus of the same specimen, CRP3-57.71-.72 mbsf. Figure 7-8. *Stephanopyxis* sp. 3; (7) High/middle/low focus of the same specimen, CRP3-54.19-.20 mbsf; (8) High/low focus of the same specimen, CRP3-37.29-.30 mbsf.

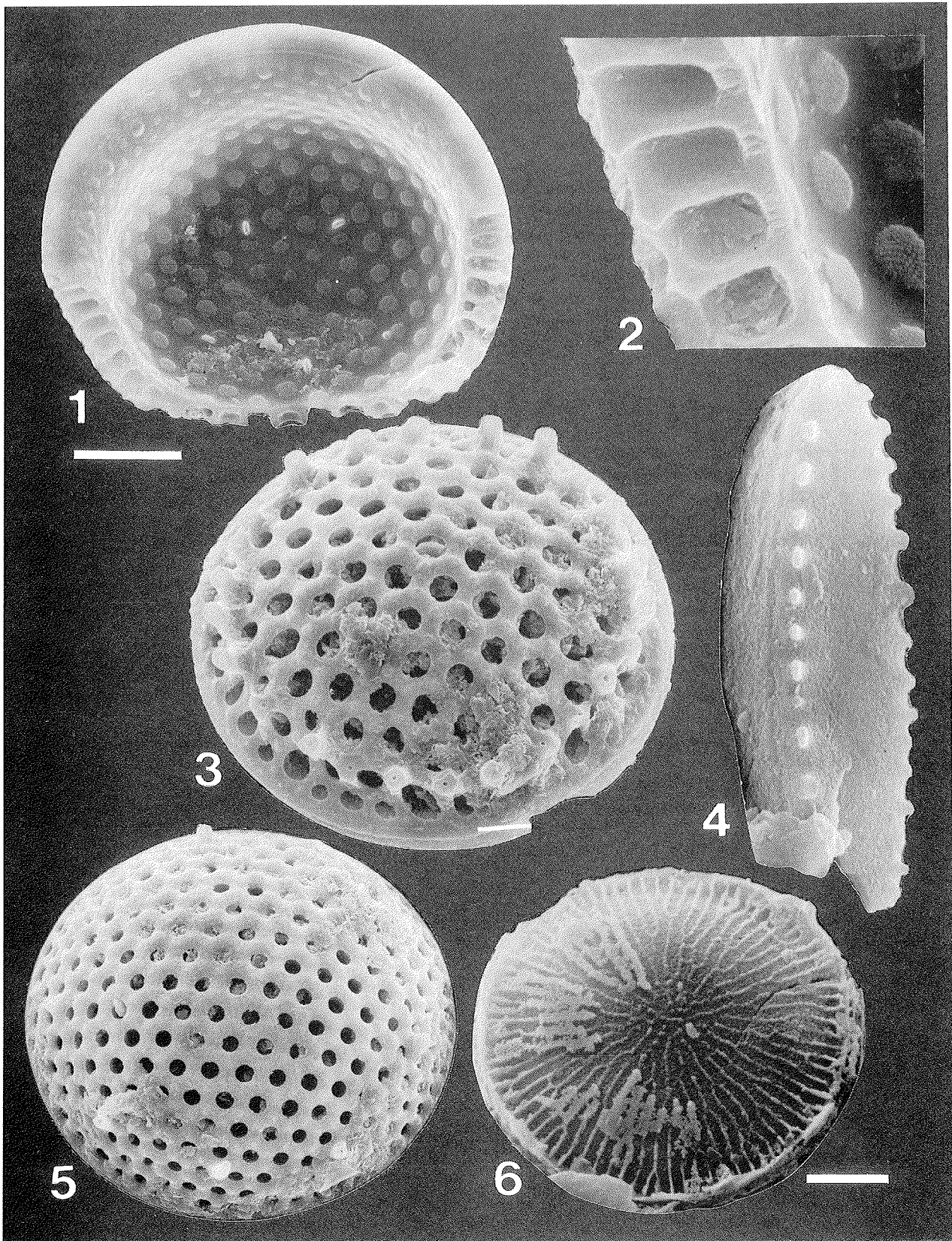


Plate 9 - SEM photomicrographs. Scale bar for figs. 1, 3, 5 (upper left) equals 10  $\mu\text{m}$ ; scale bar for figures 2, 4, 6 9 (lower right) equals 2  $\mu\text{m}$ .

Figures 1-2. *Stephanopyxis* sp. 5; (1) Internal view of valve, CRP3-43.70-.72 mbsf; (2) Close-up of wall structure for specimen shown in fig. 1. Figure 3. *Stephanopyxis* sp. cf. *S. superba* (Greville) Grunow. CRP3-43.70-.72 mbsf. Figure 4. *Ikebea* sp. D; CRP3-57.80-.81 mbsf. Figure 5. *Stephanopyxis* sp. 8; CRP3-43.70-.72 mbsf. Figure 6. *Skeletonemopsis mahoodii* Sims; CRP3-57.80-.81 mbsf.

- Stephanopyxis turris* (Greville & Arnott) Ralfs in Pritchard. (Pl. 6, Figs. 12-15)
- Stephanopyxis spp.** Comments: Taxa included commonly in *Stephanopyxis* spp. are abundant in CRP-3 samples. Many morphologies are present, which we have tentatively attempted to split into several informal groups. Further SEM work is required to identify the structure and positions of valve processes to clarify these divisions and better understand the taxonomic placement in recently proposed genera *Stephanonycites*, *Eustephanias*, *Dactylacanthis* of Komura (1999). These genera were unknown to the authors at the time of data collection for CRP-3. Related taxa reported from other drillcores in the western Ross Sea will also need to be evaluated in future studies. Comments are given below to help guide future work in resolving these taxa. *Stephanopyxis* sp. B of Harwood, 1986, pl. 14, fig. 5 could be *Stephanonycites variegates* Komura, and *Pyxilla* sp. A of Harwood, 1989, pl. 1, figs. 21-25 is likely a species of *Eustephanias*. (Plate 7, Fig. 2)
- Stephanopyxis sp. 1** Description: Valve face circular, low convex dome; regular hexagonal areolae (2.5 to 3 in 10  $\mu\text{m}$ ) arranged in regular tangential rows across the valve face; margin hyaline, 1-2  $\mu\text{m}$  in width; ring of marginal spines (1 in 15–20  $\mu\text{m}$ ). In LM, a circular line around the valve is visible below the inner edge of the outermost ring of areolae in some focal planes. This line reflects the interior edge of a broad marginal zone. (Pl. 8, Figs. 1-4)
- Stephanopyxis sp. 2** Description: Valve cylindrical to spherical; areolae hexagonal of variable size on valves of the same frustule (3 in 10  $\mu\text{m}$  and 4-5 in 10  $\mu\text{m}$ ); ring of long spines, often broken, arise vertically from the valve shoulder. Remarks: This diatom should be placed within *Dactylacanthis* Komura (1999), pending further SEM study. (Pl. 6, Fig. 16, 21)
- Stephanopyxis sp. 3** Description: Valve face circular, hemispherical, with steep mantle; hexagonal areolae (3 in 10  $\mu\text{m}$ ) arranged in tangential rows across valve face and mantle; cross-sectional structure of areolae visible in LM across the steep mantle. In LM, a circular line around the valve is visible beneath the inner edge of the outermost ring of areolae, and the most distinctive character is the optical effect that produces a diffuse circular area in the center of the valve, when the focal plane is on the base of the valve, as clearly visible in the illustrated specimens; this diffuse circular area may be off-center if the valve is tilted. This optical effect is enhanced by closing the condenser diaphragm. Under high magnification, this appears to be created by the presence of a thin siliceous septa that extends 2 to 3  $\mu\text{m}$  toward the center of the valve, at a level parallel to the valve base. (Pl. 7, Figs. 4, 6; Pl. 8, Fig. 5)
- Stephanopyxis sp. 4** Description: Frustule ovoid in girdle view comprised of two circular valves; areolae hexagonal (7 in 10  $\mu\text{m}$ ) arranged in close packing tangential rows; valve face and mantle covered with dense small spines, longer on the valve face. Remarks: This taxon likely belongs in genus *Stephanonycites*, near *S. variegates*. (Pl. 6, Figs. 19-20)
- Stephanopyxis sp. 5** Valve hemispherical with steep mantle; regular hexagonal areolae (3.5 in 10  $\mu\text{m}$  at the valve center and 5 in 10  $\mu\text{m}$  at the margin) arranged in close-packed tangential rows; 2 to 5 labiate processes are present at the valve apex within 2 to 4 areolae from the valve center. Remarks: This taxon should be included within genus *Eustephanias* Komura (1999), and several species of *Eustephanias* were likely included here, including *E. quasinermus* and *E. inermis*. (Pl. 7, Fig. 1; Pl. 9, Figs. 1-2)
- Stephanopyxis sp. 6** Description: Valve circular, slightly convex, often with flat central area; hexagonal areolae (6-7 in 10  $\mu\text{m}$ ) arranged in tangential rows, decreasing in size toward the margin; valve surface sparsely ornamented with short spines, and often bearing a central ring of small spines at 1/3 valve radius, near the edge of the flat central area; margin, hyaline and narrow (1-2  $\mu\text{m}$ ). Remarks: This diatom appears close to genus *Stephanonycites*, nearer to *S. coronus* Komura than to other species. (Pl. 8, Figs. 7, 8)
- Stephanopyxis sp. 7** (Pl. 6, Fig. 11)
- Stephanopyxis sp. 8** Remarks: No apical processes were noted in this diatom, but a ring of short spines/external tubes of processes occurs near the margin. (Pl. 7, Figs. 3, 5; Pl. 9, Fig. 5)
- Stephanopyxis sp. 9** Remarks: This small diatom is distinguished by the heterovalvate valves of different size on a single frustule. (Pl. 6, Figs. 17-18)
- Stephanopyxis sp. 10** (Pl. 8, Fig. 6)
- Stictodiscus hardmanianus* Greville; Harwood, 1989, p. 81, pl. 1, fig. 6; Scherer et al., 2000, p. 440, pl. 6, fig. 4.
- Stictodiscus? kittonianus* Greville; Harwood, 1989, p. 81, pl. 1, figs. 7-8; Barron & Mahood, 1993, p. 44, pl. 2, fig. 8. Remarks: As noted by Komura (1999) this diatom may belong within the recently proposed genus *Stictolecanon* Komura, 1999, p. 42-46, but SEM analysis is needed to verify this taxonomic position. (Pl. 2, Figs. 1-2)
- Thalassiosira? mediaconvexa* Schrader & Fenner, 1976, pl. 36, fig. 1; Barron & Mahood, pl. 4, fig. 9, 12; Scherer & Koç, 1996, p. 89, pl. 4, figs. 8-9. (Pl. 2, Figs. 3-4)
- Triceratium pulvinar* Schmidt.
- Trigonium arcticum* (Brightwell) Cleve.
- Trinacria excavata* Heiberg; Scherer et al., 2000, pl. 4, fig. 8; pl. 6, fig. 5.
- Trinacria racovitzae* Van Heurck; Harwood, 1986a, p. 87, pl. 5, figs. 2-6; Scherer et al., 2000, p. 440, pl. 4, figs. 6, 10-11.
- Trochosira spinosus* Kitton; Scherer et al., 2000, p. 440, pl. 2, figs. 4-6.
- Vulcanella hanna* Sims & Mahood, 1998, p. 115, figs. 1-12, 44-48; *Cotyledon fogedi* (Hendey) Harwood, 1989; *Tumulopsis fogedi* Hendey *sensu* Barron & Mahood, 1993 p. 44, pl. 2, figs. 7, 9, 10. (Pl. 5, Fig. 9)
- Genus et species indet. A** of Harwood, 1989, p. 82, pl. 1, figs. 9-13.
- Genus et species indet. B** of Harwood, 1989, p. 82, pl. 1, figs. 14-16.
- Genus et species indet. C** of Harwood, 1989, p. 82, pl. 3, figs. 32-33. (Pl. 5, Figs. 10-11)
- Genus et species indet.** (Pl. 1, Fig. 27)

## SILICOFLAGELLATES

*Corbisema apiculata apiculata* (Lemmermann) Hanna.

*Corbisema triacantha* (Ehrenberg) Hanna.

*Dictyocha deflandrei* Frenguelli ex Glezer.

*Dictyocha frenguelli* Deflandre.

*Dictyocha* spp.

*Distephanus crux* (Ehrenberg) Dumitrica.

*Distephanus raupii* Bukry.

## EBRIDIAN

*Ammodoichium rectangulare* (Schulz) Deflandre; Bohaty & Harwood, 2000, p. 121-122, pl. 1, figs. 2, 3; pl. 3, figs. 4-8; pl. 4, figs. 7-8; pl. 5, fig. 9; pl. 9, fig. 11; pl. 10, fig. 14.

*Falsebria ambigua* Deflandre / *Hovasebria brevispinosa* (Hovasse) Deflandre group; Scherer et al., 2000, pl. 6, figs. 8-10; Bohaty & Harwood, 2000, p. 125, p. 126, pl. 5, fig. 5.

*Micromarsupium* sp. cf *M. curticanuum* Deflandre; Bohaty & Harwood, 2000, p. 130, pl. 5, fig. 8; pl. 6, figs. 1-2, 5.

*Pseudammodoichium sphericum* Hovasse; Bohaty & Harwood, 2000, p. 134, pl. 5, fig. 6; pl. 10, figs. 7-8. Comments: Both single and double-skeleton morphologies of *Pseudammodoichium sphericum* are noted in the CRP-3 drillcore.

## ENDOSKELETAL DINOFLAGELLATES

*Cardiifolia gracilis* Hovasse; Bohaty & Harwood, 2000, p. 151, pl. 4, fig. 1.

*Calicipedinium* sp. A of Scherer et al., 2000, p. 440-441, pl. 5, fig. 8.

## CHRYSOPHYTE CYSTS

*Archaeosphaeridium australensis* Perch-Nielsen; Bohaty & Harwood, 2000, p. 150, pl. 10, fig. 11.

*Archaeosphaeridium tasmaniae* Perch-Nielsen; Bohaty & Harwood, 2000, p. 150, pl. 10, figs. 12, 18. (Pl. 5, Fig. 7)

*Archaeosphaeridium edwardsii* Perch-Nielsen; Harwood, 1989, p. 82, pl. 6, fig. 13.

ACKNOWLEDGEMENTS - Support for the Cape Roberts Project comes from the international consortium consisting of the national research programs of Australia, Germany, Italy, US, New Zealand, United Kingdom and United States. Support for this research came from NSF grant OPP-9420062. J. Barron, J. Fenner and A. Gladenkov provided helpful comments in review. We offer our thanks to V. Thorn for technical assistance in the darkroom, to D. Watkins for noting diatom occurrences in nannofossil preparations, to D. Winter for SEM photomicrographs, and to R. Scherer for helpful discussions. We applaud the excellent studies by S. Komura to document the morphological structures of many diatoms that now seem less problematic as a result of his fine work.

## REFERENCES

Akiba F., Hiramatsu C. & Yanagisawa Y., 1993. A Cenozoic diatom genus *Cavitatus* Williams; an emended description and two new biostratigraphically useful species, *C. lanceolatus* and *C.*

*rectus* from Japan. *Bull. Natn. Sci. Mus., Tokyo*, Ser. C, **19**, 11-39.

Baldauf J.G. & Barron J.A., 1991. Diatom biostratigraphy: Kerguelen Plateau and Prydz Bay regions of the Southern Ocean. In: Barron J.A., Larsen B. et al. (eds.), *Proceedings of the Ocean Drilling Program, Scientific Results*, College Station, TX (Ocean Drilling Program), **119**, 547-598.

Barron J.A., Baldauf J.G., Barrera E., Caulet J.-P., Huber B.T., Keating B.H., Lazarus D., Sakai H., Thierstein H.R. & Wei W., 1991. Biochronologic and magnetostratigraphic synthesis of Leg 119 sediments from the Kerguelen Plateau and Prydz Bay, Antarctica. In: Barron J.A., Larsen B. et al. (eds.), *Proceedings of the Ocean Drilling Program, Scientific Results*, College Station, TX (Ocean Drilling Program), **119**, 813-847.

Barron J.A. & Mahood A.D., 1993. Exceptionally well-preserved early Oligocene diatoms from glacial sediments of Prydz Bay, East Antarctica. *Micropalaeontology*, **39**, 29-45.

Berggren W.A., Kent D.V., Swisher C.C. III & Aubry M.-P., 1995. A revised Cenozoic geochronology and chronostratigraphy. In: Berggren W.A., Kent D.V., Aubry M.-P. & Hardenbol J.A. (eds.), *Geochronology, Time Scales, and Global Stratigraphic Correlation*, SEPM Special Publication, **54**, 129-212.

Bohaty S.M. & Harwood D.M., 2000. Ebridian and silicoflagellate biostratigraphy from Eocene McMurdo erratics and the Southern Ocean. In: Stilwell J.D. & Feldmann R.M. (eds.), *Palaeobiology and Palaeoenvironments of Eocene Fossiliferous Erratics, McMurdo Sound, Antarctica*, Antarctic Research Series, American Geophysical Union, **76**, 99-159.

Cape Roberts Science Team, 2000. Studies from the Cape Roberts Project, Ross Sea, Antarctica: Initial Report on CRP-3. *Terra Antarctica*, **7**, 1-209.

Ciesielski P.F., 1975. Biostratigraphy and palaeoecology of Neogene and Oligocene silicoflagellates from cores recovered during Antarctic Leg 28, Deep Sea Drilling Project. In: *Initial Reports of the Deep Sea Drilling Project*, edited by D.E. Hayes, L.A. Frakes et al., U.S. Government Printing Office, Washington, D.C., **28**, 625-691.

Ciesielski P.F., 1991. Biostratigraphy of diverse silicoflagellate assemblages from the early Palaeocene to early Miocene of Holes 698A, 700B, 702B, and 703A: subantarctic South Atlantic. In: *Proceedings of the Ocean Drilling Program, Scientific Results*, edited by P.F. Ciesielski, Y. Kristoffersen et al., College Station, Texas (Ocean Drilling Program), **114**, 49-96.

Fenner J., 1984. Eocene-Oligocene planktic diatom stratigraphy in the low latitudes and the high southern latitudes. *Micropalaeontology*, **30**, 319-342.

Fenner J., 1985. Late Cretaceous to Oligocene planktic diatoms. In: Bolli H.M., Saunders J.B. & Perch-Nielsen K. (eds.), *Plankton Stratigraphy*, Cambridge University Press, pp. 713-762.

Fenner J., 1994. Diatoms of the Fur Formation, their taxonomy and biostratigraphic interpretation. - Results from the Harre borehole, Denmark. *Aarhus Geoscience*, **1**, 99-163.

Florindo F., Wilson G.S., Roberts A.P., Sagnotti L. & Verosub K.L., 2001. Magnetostratigraphy of late Eocene - early Oligocene strata from the CRP-3 core, Victoria Land Basin, Antarctica. This volume.

Gladenkov A.Y., 1998. Oligocene and lower Miocene diatom zonation in the North Pacific. *Stratigraphy and Geological Correlation (Stratigrafiya, Geologicheskaya Korrelyatsiya)*, **6**, 150-164.

Gladenkov A.Y. & Barron J.A., 1995. Oligocene and early middle Miocene diatom biostratigraphy of Hole 884B. In: Rea D.K., Basov I.A., Scholl D.W. & Allan J.F. (eds.), *Proceedings of the Ocean Drilling Program, Scientific Results*, College Station, TX (Ocean Drilling Program), **145**, 21-41.

Gombos A.M. Jr., 1977. Palaeogene and Neogene diatoms from the Falkland Plateau and Malvinas Outer Basin. In: Barker P.F., Dalziel I.W.D. et al. (eds.), *Initial Reports of the Deep Sea Drilling Project*, Washington, U.S. Government Printing Office, **36**, 575-687.

Gombos A.M. Jr. & Ciesielski P.F., 1983. Late Eocene to early Miocene diatoms from the southwest Atlantic. In: Ludwig W.J., Krasheninikov V.A. et al. (eds.), *Initial Reports of the Deep Sea Drilling Project*, Washington (U.S. Government Printing Office), **71**, 583-634.

- Hajós M., 1976. Upper Eocene and lower Oligocene diatomaceae, archaomonadaceae, and silicoflagellatae in southwestern Pacific sediments, DSDP Leg 29. In: Hollister C.D., Craddock C. et al. (eds.), *Initial Reports of the Deep Sea Drilling Project*, Washington, U.S. Government Printing Office, **35**, 817-884.
- Hannah M.J., 1997. Climate controlled dinoflagellate distribution in late Eocene-earliest Oligocene strata from CIROS-1 drillcore, McMurdo Sound, Antarctica. *Terra Antarctica*, **4**, 73-78.
- Harwood D.M., 1986. Diatoms. In: Barrett P.J. (ed.), *Antarctic Cenozoic History from the MSSTS-1 Drillhole, McMurdo Sound*, *DSIR Bulletin*, **237**, 69-107.
- Harwood D.M., 1989. Siliceous microfossils. In: Barrett P.J. (ed.), *Antarctic Cenozoic History from the CIROS-1 Drillhole, McMurdo Sound*, *DSIR Bulletin*, **245**, 67-97.
- Harwood D.M., 1994. Correlating Antarctic marine and terrestrial sediments by marine diatoms. In: van der Wateren F.M., Verbers A.L.L.M. & Tessensohn F. (eds.), *LIRA Workshop on Landscape Evolution, an interdisciplinary approach to the relationship between Cenozoic climate change and tectonics in the Ross Sea area*. Rijks Geologische Dienst, Haarlem, Nederland, 97-100.
- Harwood D.M., Barrett P.J., Edwards A.R., Rieck H.J. & Webb P.-N., 1989a. Biostratigraphy and chronology. In: Barrett P.J. (ed.), *Antarctic Cenozoic History from the CIROS-1 Drillhole, McMurdo Sound*, *DSIR Bulletin*, **245**, 231-239.
- Harwood D.M., Scherer R.P. & Webb P.-N., 1989b. Multiple Miocene productivity events in West Antarctica as recorded in upper Miocene sediments beneath the Ross Ice Shelf (Site J-9). *Marine Micropaleontology*, **15**, 91-115.
- Harwood D.M., Lazarus D., Abelman A., Aubry M.P., Berggren W.A., Heider F., Inokuchi H., Maruyama T., McCartney K., Wei W., & Wise S.W. Jr., 1992. Neogene integrated magnetobiostratigraphy of the Southern Kerguelen Plateau, ODP Leg 120. *Proceedings of the Ocean Drilling Program, Science Results*, **120**, 1031-1052.
- Harwood D.M. & Maruyama T., 1992. Middle Eocene to Pleistocene diatom biostratigraphy of Southern Ocean sediments from the Kerguelen Plateau, Leg 120. In: Wise S.W. Jr., Schlich R. et al. (eds.), *Proceedings of the Ocean Drilling Program, Scientific Results*, College Station, TX, Ocean Drilling Program, **120**, 683-733.
- Harwood D.M. & Bohaty S.M., 2000. Marine diatom assemblages from Eocene and younger erratics, McMurdo Sound, Antarctica. In: Stilwell J.D. & Feldmann R.M. (eds.), *Palaeobiology and Palaeoenvironments of Eocene Fossiliferous Erratics, McMurdo Sound, Antarctica*, Antarctic Research Series, American Geophysical Union, **76**, 73-98.
- Harwood D.M., Bohaty S.M. & Scherer R.P., 1998. Lower Miocene Diatom Biostratigraphy of the CRP-1 Drillcore, McMurdo Sound, Antarctica. *Terra Antarctica*, **5**, 499-514.
- Komura S., 1980. A new genus of cuneate diatom from the Miocene Masuporo Formation of the Tenpoku district, Japan. Professor Saburo Kanno Memorial Volume. Tsukuba, Japan: Tsukuba Univ. Press. 373-378.
- Komura S., 1996. An attachment mode of opposite valves in some diatom frustules. *Diatom*, **12**, 7-26.
- Komura S., 1999. Further observations on valve attachment within diatom frustules and comments on several new taxa. *Diatom*, **15**, 11-50.
- Mahood A.D., Barron J.A. & Sims P.A., 1993. A study of some unusual, well-preserved Oligocene diatoms from Antarctica. *Nova Hedwigia, Beiheft*, **106**, 243-267.
- McCartney K., & Harwood D.M., 1992. Silicoflagellates from Leg 120 on the Kerguelen Plateau, southeast Indian Ocean. In: *Proceedings of the Ocean Drilling Program, Scientific Results*, edited by S.W. Wise, Jr., R. Schlich et al., College Station, Texas (Ocean Drilling Program), **120** (part 2), 811-831.
- McCartney K. & Wise S.W. Jr., 1990. Cenozoic silicoflagellates and ebridians from ODP Leg 113: biostratigraphy and notes on morphologic variability. In: P.F. Barker, J.P. Kennett et al. (eds.) *Proceedings of the Ocean Drilling Program, Scientific Results*, College Station, Texas (Ocean Drilling Program), **113**, 729-760.
- McCollum D.W., 1975. Diatom stratigraphy of the Southern Ocean. In: Hayes D.E., Frakes L.A. et al. (eds.), *Initial Reports of the Deep Sea Drilling Project*, Washington, U.S. Govt. Printing Office, **28**, 515-571.
- McMinn, A., 1995. Why are there no post-Palaeogene dinoflagellate cysts in the Southern Ocean? *Micropaleontology*, **41**, 383-386.
- Perch-Nielsen K., 1975a. Late Cretaceous to Pleistocene archaemonads, ebridians, endoskeletal dinoflagellates, and other siliceous microfossils from the subantarctic southwest Pacific, DSDP, Leg 29. In *Initial Reports of the Deep Sea Drilling Project*, edited by J.P. Kennett, R.E. Houtz et al., U.S. Government Printing Office, Washington, D.C., **29**, 873-907.
- Perch-Nielsen K., 1975b. Late Cretaceous to Pleistocene silicoflagellates from the southern southwest Pacific, DSDP, Leg 29. In: *Initial Reports of the Deep Sea Drilling Project*, edited by J.P. Kennett, R.E. Houtz et al., U.S. Government Printing Office, Washington, D.C., **29**, 677-721.
- Ramsay A.T.S. & Baldauf J.G., 1999. *A Reassessment of the Southern Ocean Biochronology*. Geological Society, London, Memoir **18**, 122 p.
- Scherer R.P. & Koç N., 1996. Late Palaeogene diatom biostratigraphy and palaeoenvironments of the northern Norwegian-Greenland Sea. In: Thiede J., Myhre A.M., Firth J.V., Johnson G.L., & Ruddiman W.F. (eds.), *Proceedings of the Ocean Drilling Program, Scientific Results*, College Station, TX, Ocean Drilling Program, **151**, 75-99.
- Scherer R.P., Bohaty S.M. & Harwood D.M., 2000. Oligocene and lower Miocene siliceous microfossil biostratigraphy of Cape Roberts Project Core CRP-2/2A, Victoria Land Basin, Antarctica. *Terra Antarctica*, **7**, 417-442.
- Schrader H.-J. 1976. Cenozoic planktonic diatom biostratigraphy of the Southern Pacific Ocean. In: Hollister C.D., Craddock C. et al. (eds.), *Initial Reports of the Deep Sea Drilling Project*, Washington, U.S. Govt. Printing Office, **35**, 605-672.
- Schrader H.-J. & Fenner J., 1976. Norwegian Sea Cenozoic diatom biostratigraphy and taxonomy. In: Talwani M., Udintsev G. et al. (eds.), *Initial Reports of the Deep Sea Drilling Project*, Washington, U.S. Government Printing Office, **38**, 921-1099.
- Sheshukova V.S., 1962. New and rare Bacillariophyta from the diatom suite of Sakhalin. *Uchenyye Zapiski of Leningrad State University, Seriya Biologicheskii Nauk*, **49**(313), 203-211. (In Russian)
- Sims P.A., 1986. *Sphinctoletus* Hanna, *Ailuretta* gen. nov., and evolutionary trends within the Hemiauloideae. *Diatom Research*, **1**, 241-269.
- Sims P. A., 1994. *Skeletonemopsis*, a new genus based on the fossil species of the genus *Skeletonema* Grev. *Diatom Research*, **9**, 387-410.
- Sims P. A. & Mahood A., 1998. *Vulcanella hanna* Sims and Mahood, gen. et sp. nov., with a discussion of the genera *Tumulopsis* Hendy, *Acanthodiscus* Pantocsek, *Poretzkia* Jouse and *Goniothecium* Ehrenberg. *Diatom Research*, **13**, 113-131.
- Steinhauff D.M., Renz M.E., Harwood D.M. & Webb P.N., 1987. Miocene diatom biostratigraphy of DSDP Hole 272: stratigraphic relationship to the underlying Miocene of DSDP Hole 270, Ross Sea, Antarctica. *Antarctic Journal of the U.S.*, **22**, 123-125.
- Wei W. & Wise S.W. Jr., 1992. Oligocene-Pleistocene calcareous nannofossils from Southern Ocean Sites 747, 748, and 751. *Proceedings of the Ocean Drilling Program, Scientific Results*, **120**, 509-522.
- White R.J., 1980. Southern Ocean silicoflagellate and ebridian biostratigraphy, the opening of the Drake Passage, and the Miocene of the Ross Sea, Antarctica, Northern Illinois University, DeKalb, Illinois, Master's Thesis, 205 pp.
- Wilson, G.J., 1989. Marine palynology. In: Barrett P.J. (ed.), *Antarctic Cenozoic History from the CIROS-1 Drillhole, McMurdo Sound*, *DSIR Bulletin*, **245**, 129-134.
- Wilson G.S., Bohaty S.M., Fielding C.R., Florindo F., Hannah M.J., Harwood D.M., McIntosh W.C., Naish T.R., Roberts A.P., Sagnotti L., Scherer R.P., Strong C.P., Verosub K.L., Villa G., Watkins D.K., Webb P.-N. & Woolfe K.J., 2000. Chronostratigraphy of the CRP-2/2A Drillhole, Ross Sea, Antarctica. *Terra Antarctica*, **7**, 647-654.
- Yanagisawa Y. & Akiba F., 1998. Refined Neogene diatom biostratigraphy for the northwest Pacific around Japan, with an introduction of code numbers for selected diatom biohorizons. *The Journal of the Geological Society of Japan*, **104**, 395-414.